# Theory of Excited State Decays and Optical Spectra: Application to Polyatomic Molecules

**Yingli Niu,[†] Qian Peng,[†] Chunmei Deng, Xing Gao,[‡] and Zhigang Shuai*,[†,‡]**

*Key Laboratory of Organic Solids, Beijing National Laboratory for Molecular Sciences (BNLMS), Institute of Chemistry, Chinese Academy of Sciences, 100190 Beijing, People's Republic of China, and Department of Chemistry, Tsinghua University, 100084 Beijing, People's Republic of China*

General formalism of absorption and emission spectra, and of radiative and nonradiative decay rates are derived using a thermal vibration correlation function formalism for the transition between two adiabatic electronic states in polyatomic molecules. Displacements, distortions, and Duschinsky rotation of potential energy surfaces are included within the framework of a multidimensional harmonic oscillator model. The Herzberg–Teller (HT) effect is also taken into account. This formalism gives a reliable description of the $Q_x$ spectral band of free-base porphyrin with weakly electric dipole-allowed transitions. For the strongly dipole-allowed transitions, e.g., $S_1 \rightarrow S_0$ and $S_0 \rightarrow S_1$ of linear polyacenes, anthracene, tetracene, and pentacene, the HT effect is found to enhance the radiative decay rates by ~10% compared to those without the HT effect. For nonradiative transition processes, a general formalism is presented to extend the application scope of the internal conversion theory by going beyond the promoting-mode approximation. Numerical calculations for the nonradiative $S_1 \rightarrow S_0$ decay rate of azulene well explain the origin of the violation of Kasha's rule. When coupled with first-principles density functional theory (DFT) calculations, the present approach appears to be an effective tool to obtain a quantitative description and detailed understanding of spectra and photophysical processes in polyatomic molecules.

## I. Introduction

Optical absorption, emission, and nonradiative processes in molecules are of both fundamental[1−4] and applied interests.[5−7] In organic light-emitting materials, the emission color is determined by both the electronic transition energy from the excited state to the ground state and the vibrationally resolved emission spectrum.[8] The light-emitting efficiency is determined by a competition between radiative and nonradiative decay rates. In general, molecular aggregation quenches emission due to intermolecular charge or energy transfer, or the formation of H-type aggregates. However, recently, it has been found that some molecules,[9−18] such as siloles, present aggregation induced or enhanced light-emission phenomena, which is highly desirable for materials science since, in practical application, molecular materials are found in solid film state, which are expected to efficiently emit light. This finding has inspired strong interests in quantitative descriptions for radiative and nonradiative decay processes in organic molecular light-emitting materials.[19−28] Yin et al.[21] first applied a linear coupling model (LCM)[29] to calculate and to analyze the vibronic coupling factors for two types of silole molecules, to get insight into the intramolecular nonradiative decay processes. This work has accounted for aggregation induced emission (AIE) in silole as well as the steric hindrance effect. It is noted that when potential energy surfaces (PES) intercross, i.e., the conical intersections (CIs)[30] occur, the nonradiative decay process could be very efficient, which could be important in describing the light-emitting processes, especially for molecules in gas phase or in solution.
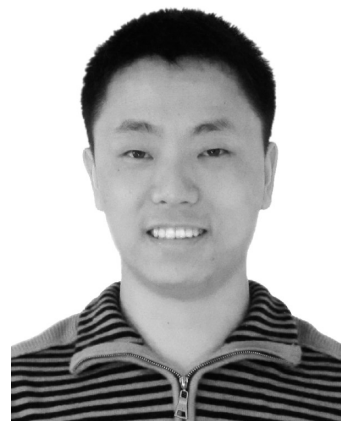
**Yingli Niu** graduated with his B.S. degree in physics from Northeast Normal University, in 2003, and received his M.S. degree in condensed matter physics from Jilin University under the supervision of Prof. Yanming Ma in 2007. Then he studied in Prof. Zhigang Shuai's group at the Institute of Chemistry, Chinese Academy of Sciences (CAS) and obtained his Ph.D. degree in physical chemistry in 2010. His research interests are focused on molecular vibrational spectra and excited state nonradiative processes.

Nevertheless, it is usually hard to obtain the multidimensional PES of large molecules through quantum chemistry calculations. Instead, a harmonic oscillator model is typically used to approximate the PES. Within this approximation, the normal modes of the excited electronic state are mixtures of ground state modes, which is described as Duschinsky rotation.[31] To avoid the complex multidimensional integrals arising from this rotation effect, a displaced harmonic oscillator approximation has been widely used.[32−35] However, the Duschinsky rotation effect (DRE) plays an important role in many molecular systems and should not be ignored.[36−47] Barone and co-workers present an effective method to compute Franck–Condon integrals with

* Corresponding author. E-mail address: zgshuai@tsinghua.edu.cn.
† Chinese Academy of Sciences.
‡ Tsinghua University.

**Qian Peng** is a research assistant in Key Laboratory of Organic Solids, the Institute of Chemistry, CAS. She received her M.S. degree in 2004 on ''theoretical studies on some small inorganic molecular and large complex compounds'' from Northwest University, under the supervision of Prof. Zhenyi Wen, and her Ph.D. degree in 2008 on ''theoretical study on the process of excited states in isolated large organic molecules'' from the Institute of Chemistry, CAS, under the supervision of Prof. Zhigang Shuai. Her research interests are molecular excited state dynamics and opto-electronic properties of organic materials.

**Xing Gao** graduated with a M.S. degree in Chemistry from Hunan University in 2008. He is currently a graduate student in Prof. Zhigang Shuai's group at Tsinghua University. His research interest centers on excited states molecular dynamics.
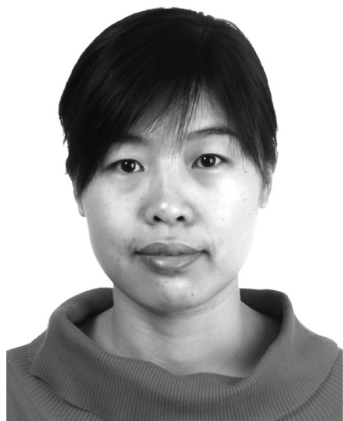
**Chunmei Deng** received her B.S. degree from Hunan Normal University in 2005, and received her M.S. degree in 2008 from Institute of Coal Chemistry, CAS, under the supervision of Prof. Haijun Jiao. She is now a Ph.D. student in Prof Zhigang Shuai's group in Institute of Chemistry, CAS. Her interest is mainly in molecular excited state dynamics and photophysical properties of organic materials.

**Zhigang Shuai** received his Ph.D. degree in 1989 from Fudan University, Shanghai. From 1990 to 2001, he worked in the University of Mons-Hainaut, Belgium, as a research scientist. From 2002, he became a professor at the Institute of Chemistry, CAS, in Beijing. Since May 2008, he is a full professor at the Department of Chemistry of Tsinghua University in Beijing. He is an elected member of the International Academy of Quantum Molecular Science (2008) and a Fellow of the Royal Society of Chemistry (2009). The major research interests in his group are theoretical modeling of organic functional opto-electronic materials and devices. He has authored or coauthored more than 200 research articles.

DRE for optical spectra of large molecules.[48,49] The method automatically selects the relevant vibronic contributions to the spectrum until the spectrum is converged. To apply this method to weakly dipole-allowed or dipole-forbidden cases, they also extended the formalism to a Herzberg−Teller (HT) expansion[50] and succeeded in describing the vibronic spectra of porphyrin. As an alternative to sum-over-states calculations, Yan and Mukamel[51] first derived a Franck−Condon integral with DRE in a Green's function formalism, and this has been further developed by Tang et al.[52] and Pollak et al.[53] in a path integral framework. The advantage of the path integral method lies in the automatic inclusion of all the vibrational states. Here, we present a unified vibration correlation function formalism for both transition rates and optical spectra that includes both DRE and HT effects. In the case of the radiationless decay rate, the promoting mode assumption is abandoned, allowing for a more general description of polyatomic molecules.

We previously developed an analytic formalism for the internal conversion (IC) rate that includes DRE for multimode mixing,[23,24] based on the radiationless process theory developed by Lin et al.[19,20,54−57] This approach gave a reasonable temperature dependence for the IC rate of tetraphenylbutadiene isomers and highlighted the important role played by the mixing of low-frequency phenyl ring twisting modes, which is the key to understand the aggregation induced emission phenomena. Namely, electrons in the conjugation backbone are loosely coupled with side ring twisting motions that dissipate efficiently the electron excitation energy and, at the same time, the side rings tend to protect the backbone from intermolecular luminescence quenching. However, this approach relied on a promoting-mode formalism that made two key assumptions: (i) (only) one specific vibrational mode, called the promoting mode, is isolated from all other modes and this is the only mode that contributes to the electronic coupling prefactor, and (ii) this promoting mode in the final electronic state is not displaced, distorted, or mixed with other modes in the initial electronic state. Later, we removed these two limitations and presented a promoting-mode free formalism, which includes the contribution of all normal modes to the electronic coupling and thereby completely avoids the problems associated with mode selection and with finding modes correspondence.[25] This formalism has

Feature Article

*J. Phys. Chem. A, Vol. 114, No. 30, 2010* **7819**

been successfully applied in the calculations of the polyatomic optical spectra and excited state decay rates in our previous work.[27,28,58]

It has to be noted that such an approach did not take the conical intersection into account; thus the application scope is limited to situations where the photophysical processes occur at points away from any potential energy surface crossing. In fact, for polyatomic molecules, the multidimensional harmonic oscillator description is practical, and probably relevant. In this article, we give a comprehensive description of these developments and present new application examples of the formalism, coupled with quantum chemical calculations, to some polyatomic molecules that have interesting photophysical properties. In section II, we report the general formalism for absorption and emission spectra with DRE and Herzberg–Teller expansion. Section III presents the formalism for radiative and nonradiative transition rates. Section IV describes the computational details and Section V gives some application examples. Finally, we give some perspectives in section VI.

## II. Optical Spectroscopy Formalism

**A. Harmonic Oscillator Model.** Suppose a transition (absorption, emission, or nonradiative decay) happens between initial vibronic state $|\Psi_{iv_i}\rangle = |\Phi_i\Theta_{iv_i}\rangle$ and final vibronic state $|\Psi_{fv_f}\rangle = |\Phi_f\Theta_{fv_f}\rangle$. Here we apply the Born–Oppenheimer approximation, on which the vibronic states $|\Psi_{iv_i}\rangle$ and $|\Psi_{fv_f}\rangle$ are described by the products of the electronic states $|\Phi_i\rangle$, $|\Phi_f\rangle$ and the vibrational states $|\Theta_{iv_i}\rangle$, $|\Theta_{fv_f}\rangle$. Throughout this paper, the letters i and f are used only as labels of the initial and the final electronic states, respectively. And the corresponding vibrational quantum numbers are denoted by $v_i$ and $v_f$. Under the harmonic PES approximation, the molecular vibrational state is composed of $N$ independent harmonic oscillator states, $|\Theta_{iv_i}\rangle = |\chi_{iv_{i1}}\chi_{iv_{i2}}\cdots\chi_{iv_{iN}}\rangle$ and $|\Theta_{fv_f}\rangle = |\chi_{fv_{f1}}\chi_{fv_{f2}}\cdots\chi_{fv_{fN}}\rangle$. Here, $v_i = \{v_{i1}, v_{i2}, ..., v_{iN}\}$ and $v_f = \{v_{f1}, v_{f2}, ..., v_{fN}\}$, which we have defined as the vibrational quantum numbers. For molecule with $n$ atoms, there are $N = 3n - 6$ (or $N = 3n - 5$ for linear molecule) normal modes. $|\chi_{iv_{ik}}\rangle$ and $|\chi_{fv_{fk}}\rangle$ are eigenstates of the 1-dimensional harmonic oscillator Hamiltonian:

$$\hat{H}_{ik} = \frac{1}{2}(\hat{P}_{ik}{}^2 + \omega_{ik}{}^2\hat{Q}_{ik}{}^2) \tag{1}$$

$$\hat{H}_{fl} = \frac{1}{2}(\hat{P}_{fl}{}^2 + \omega_{fl}{}^2\hat{Q}_{fl}{}^2) \tag{2}$$

$\hat{P}_k$ and $\hat{Q}_k$ are the $k$th mass-weighted nuclear normal momentum operator and normal coordinate operator. The eigenvalue is $E_k = (v_k + 1/2)\hbar\omega_k$. The normal mode coordinates $Q_{ik}$ and $Q_{fl}$ can be represented by mass-weighted Cartesian coordinates,

$$Q_{ik} = \sum_{\sigma=1}^{n} \sum_{j=x,y,z} L_{i\sigma j,k}(q_{i\sigma j} - q_{i\sigma j}^0) \tag{3}$$

$$Q_{fl} = \sum_{\sigma=1}^{n} \sum_{j=x,y,z} L_{f\sigma j,l}(q_{f\sigma j} - q_{f\sigma j}^0) \tag{4}$$

Here $\sigma$ is the index for nuclei, and $j = x, y, z$ represents the Cartesian component. $q_{\sigma j}$ is the mass-weighted Cartesian coordinate of nucleus $\sigma$. The superscript 0 in $q_{i\sigma j}^0$ and $q_{f\sigma j}^0$ denotes

the equilibrium position of molecular structure in the initial or final electronic state.

The electronic transition and subsequent vibrational relaxation should not involve any additional molecular translation or rotation. We may therefore put the ground state molecular geometry and excited state molecular geometry in one frame of reference according to the following first (translational) and second (rotational) Eckart conditions,[59,60]

$$\sum_{\sigma=1}^{n} M_\sigma \mathbf{r}_{i\sigma}^0 = \sum_{\sigma=1}^{n} M_\sigma \mathbf{r}_{f\sigma}^0 = 0 \tag{5}$$

$$\sum_{\sigma=1}^{n} M_\sigma \mathbf{r}_{i\sigma}^0 \times \mathbf{r}_{f\sigma}^0 = 0 \tag{6}$$

Here $M_\sigma$ is the mass of the $\sigma$th atom. $\mathbf{r}_{i\sigma}^0$ and $\mathbf{r}_{f\sigma}^0$ are the equilibrium positions of the $\sigma$th atom in the initial and final states, respectively. First, the molecule is translated and rotated to the inertial frame of reference (the equilibrium positions are now labeled as $\mathbf{r}_{i\sigma}^{\prime 0}$ and $\mathbf{r}_{f\sigma}^{\prime 0}$) in which the first Eckart condition is automatically satisfied. Second, we set $\mathbf{r}_{f\sigma}^0 = \mathbf{r}_{f\sigma}^{\prime 0}$ and rotate the initial state geometry, $\mathbf{r}_{i\sigma}^0 = \mathbf{T}\mathbf{r}_{i\sigma}^{\prime 0}$, to meet the second Eckart condition. The pseudorotation matrix $\mathbf{T}$ can be calculated according to ref 61. After rearrangement of the two molecular equilibrium structures, the normal coordinates of the two electronic states $Q_{ik}$ and $Q_{fl}$ are related by a Duschinsky rotation matrix $\mathbf{S}_{i\leftarrow f}$ and a coordinate displacement vector $\underline{D}_{i\leftarrow f}$. Hereafter, bold variables represent square matrices and underlined variables represent column matrices.

$$Q_{ik} = \sum_{l=1}^{N} S_{i\leftarrow f,kl}Q_{fl} + \underline{D}_{i\leftarrow f,k} \tag{7}$$

where

$$\mathbf{S}_{i\leftarrow f} = \mathbf{L}_i^T\mathbf{L}_f \tag{8}$$

and

$$\underline{D}_{i\leftarrow f} = \mathbf{L}_i^T(\underline{q}_f^0 - \underline{q}_i^0) \tag{9}$$

Here $\mathbf{S}_{i\leftarrow f}$ is a unitary matrix, the Duschinsky rotation matrix, whose elements represent the mixing of normal modes in the initial and final electronic states. $\underline{D}_{i\leftarrow f}$ is a displacement vector connecting the minima of the parabolas of the two electronic states. The distortions of the final state PES correspond to the changes of the normal-mode frequencies with respected to the initial electronic state within the harmonic oscillator model. For a more elaborate description of spectra, radiative and nonradiative rates, as we will show in the following sections, the Duschinsky rotation, displacement, and distortions of PES should be included together. In the following, we will abbreviate $\mathbf{S}_{i\leftarrow f}$ and $\underline{D}_{i\leftarrow f}$ as $\mathbf{S}$ and $\underline{D}$.

**B. Optical Absorption and Emission Spectra.** The absorption spectrum is given as the absorption cross section $\sigma_{abs}(\omega)$ with dimensions of $cm^2$. This cross section is defined as the rate of photon energy absorption per molecule and per unit radiant energy flux, which is equivalent to the ratio of the power absorbed by the molecule to the incident power per unit area.

**7820** *J. Phys. Chem. A, Vol. 114, No. 30, 2010*

Niu et al.

The explicit expression for $\sigma_{abs}(\omega)$ is given by the following formula.[30,50,62]

$$\sigma_{abs}(\omega) = \frac{4\pi^2\omega}{3c} \sum_{v_i,v_f} P_{iv_i}(T) |\langle \Theta_{fv_f} | \vec{\mu}_{fi} | \Theta_{iv_i} \rangle|^2 \delta(\hbar\omega - E_{fi} - E_{fv_f} + E_{iv_i}) \quad (10)$$

Hereafter, we omit the temperature $T$ in spectra for simplicity, e.g., $\sigma_{abs}(\omega,T) \rightarrow \sigma_{abs}(\omega)$.

The emission spectrum is given as the differential spontaneous photon emission rate $\sigma_{em}(\omega)$. This is a dimensionless quantity defined as the rate of spontaneous photon emission per molecule and per unit frequency between $\omega$ and $\omega + d\omega$. The explicit expression for $\sigma_{em}(\omega)$ is given by the following formula.[30,50,62]

$$\sigma_{em}(\omega) = \frac{4\omega^3}{3c^3} \sum_{v_i,v_f} P_{iv_i}(T) |\langle \Theta_{fv_f} | \vec{\mu}_{fi} | \Theta_{iv_i} \rangle|^2 \delta(E_{if} + E_{iv_i} - E_{fv_f} - \hbar\omega) \quad (11)$$

Here $c$ is the velocity of light. $P_{iv_i}(T)$ is the Boltzmann distribution function for the initial vibronic manifold. $\vec{\mu}_{fi} = \langle \Phi_f | \vec{\mu} | \Phi_i \rangle$ is the electric transition dipole moment. $E_{fi} = E_f - E_i$ in eq 10 or $E_{if} = E_i - E_f$ in eq 11 represents the adiabatic excitation energy. $E_{iv_i}$ or $E_{fv_f}$ is the vibrational energy in the corresponding electronic state. The differential spontaneous emission power is in direct proportion to $\omega^4$,

$$I_{em}(\omega) = \sigma_{em}(\omega) \cdot \hbar\omega \propto \omega^4 \quad (12)$$

which represents the power emitted per molecule and per unit frequency between $\omega$ and $\omega + d\omega$.

Both $\sigma_{abs}(\omega)$ and $\sigma_{em}(\omega)$ possess the same form except for the dependences on $\omega$. We will use $\sigma_{em}(\omega)$ as an example to show how to derive an analytic formalism for the spectrum with an HT expansion with the thermal vibration correlation function.

In general, $\vec{\mu}_{fi}$ is not a constant vector and should depend on the nuclear coordinate. Thus it can be expanded as

$$\vec{\mu}_{fi} = \vec{\mu}_0 + \sum_k \vec{\mu}_k Q_k + \sum_{k,l} \vec{\mu}_{kl} Q_k Q_l + \ldots \quad (13)$$

For strongly dipole-allowed transitions, the spectrum is usually dominated by the zero-order term of the expansion (Franck–Condon approximation), while for weakly dipole-allowed or -forbidden transitions, one must at least consider the first order term (HT approximation).

$$\vec{\mu}_{fi} = \vec{\mu}_0 + \sum_k \vec{\mu}_k Q_k \quad (14)$$

In fact, $\vec{\mu}_k$ depends on the derivative of transition density $\rho'_k \equiv (\partial\rho_{fi}/\partial Q_k)_0$,

$$\vec{\mu}_k = \left(\frac{\partial\vec{\mu}_{fi}}{\partial Q_k}\right)_0 = -e\left(\frac{\partial \int d^3x\, \rho_{fi}\vec{r}}{\partial Q_k}\right)_0 = -e\int d^3x \left(\frac{\partial\rho_{fi}}{\partial Q_k}\right)_0 \vec{r} \equiv -e\int d^3x\, \rho'_k\vec{r} \quad (15)$$

Inserting (14) into (11), one obtains

$$\sigma_{em}(\omega) = \sigma_{em}^{FC}(\omega) + \sigma_{em}^{FC/HT}(\omega) + \sigma_{em}^{HT}(\omega) \quad (16)$$

where

$$\sigma_{em}^{FC}(\omega) = \frac{4\omega^3}{3\hbar c^3} |\vec{\mu}_0|^2 \sum_{v_i,v_f} P_{iv_i}(T) |\langle \Theta_{fv_f} | \Theta_{iv_i} \rangle|^2 \delta(\omega_{iv_i,fv_f} - \omega) \quad (17)$$

$$\sigma_{em}^{FC/HT}(\omega) = \frac{4\omega^3}{3\hbar c^3} \sum_{v_i,v_f} P_{iv_i}(T)\delta(\omega_{iv_i,fv_f} - \omega) \sum_k \vec{\mu}_0 \cdot \vec{\mu}_k \langle \Theta_{fv_f} | \Theta_{iv_i} \rangle\langle \Theta_{iv_i} | Q_{fk} | \Theta_{fv_f} \rangle \quad (18)$$

$$\sigma_{em}^{HT}(\omega) = \frac{4\omega^3}{3\hbar c^3} \sum_{v_i,v_f} P_{iv_i}(T)\delta(\omega_{iv_i,fv_f} - \omega) \sum_{k,l} \vec{\mu}_k \cdot \vec{\mu}_l \langle \Theta_{fv_f} | Q_{fk} | \Theta_{iv_i} \rangle\langle \Theta_{iv_i} | Q_{fl} | \Theta_{fv_f} \rangle \quad (19)$$

Applying the Fourier transformation to the delta-functions in the above equations:

$$\delta(\omega) = \frac{1}{2\pi} \int e^{i\omega t}\, dt \quad (20)$$

we can obtain an analytical integral formalism for the FC, FC/HT and HT spectra.

$$\sigma_{em}^{FC}(\omega) = \frac{2\omega^3}{3\pi\hbar c^3} |\vec{\mu}_0|^2 \int_{-\infty}^{\infty} e^{-i(\omega-\omega_{if})t} Z_{iv}^{-1} \rho_{em,0}^{FC}(t,T)\, dt \quad (21)$$

$$\sigma_{em}^{FC/HT}(\omega) = \frac{2\omega^3}{3\pi\hbar c^3} \sum_k \vec{\mu}_0 \cdot \vec{\mu}_k \int_{-\infty}^{\infty} e^{-i(\omega-\omega_{if})t} Z_{iv}^{-1} \rho_{em,k}^{FC/HT}(t,T)\, dt \quad (22)$$

$$\sigma_{em}^{HT}(\omega) = \frac{2\omega^3}{3\pi\hbar c^3} \sum_{k,l} \vec{\mu}_k \cdot \vec{\mu}_l \int_{-\infty}^{\infty} e^{-i(\omega-\omega_{if})t} Z_{iv}^{-1} \rho_{em,kl}^{HT}(t,T)\, dt \quad (23)$$

Here $Z_{iv}$ is the partition function, and

$$\rho_{em,0}^{FC}(t,T) = \text{Tr}[e^{-i\tau_f\hat{H}_f}e^{-i\tau_i\hat{H}_i}] \quad (24)$$

$$\rho_{em,k}^{FC/HT}(t,T) = \text{Tr}[Q_{fk}e^{-i\tau_f\hat{H}_f}e^{-i\tau_i\hat{H}_i}] \quad (25)$$

$$\rho_{em,kl}^{HT}(t,T) = \text{Tr}[Q_{fk}e^{-i\tau_f\hat{H}_f}Q_{ff}e^{-i\tau_i\hat{H}_i}] \quad (26)$$

are the three kinds of thermal vibration correlation functions. $\tau_f = t/\hbar$, $\tau_i = -i\beta - \tau_f$, and $\beta = (k_BT)^{-1}$. $k_B$ is the Boltzmann constant. To distinguish from the transition density $\rho_{fi}$ and its derivative $\rho'_k$ in (15), we use $\rho_{abs}$, $\rho_{em}$, and $\rho_{ic}$ to denote the

Feature Article

*J. Phys. Chem. A, Vol. 114, No. 30, 2010* **7821**

thermal vibration correlation functions of absorption, emission and internal conversion, respectively.

An analytical path integral formalism for the FC factor including DRE has been derived by Tang et al. in studying the DRE and temperature dependence of electron transfer processes.[63] In studying the photoinduced cooling effect for polyatomic molecules, Ianconescu and Pollak have independently derived an analytical formalism for the FC factor with DRE.[53] Along the same line, we present in Appendix A the analytical formulas for the optical absorption and emission spectra for polyatomic molecules under the displaced and distorted harmonic oscillator approximation considering both DRE and HT term, namely, compact solutions for eqs 24−26 and their counterparts for absorption.

## III. Rate Processes Formalism

**A. Radiative Decay Rate.** The radiative decay rate, i.e., the spontaneous emission rate, is simply the integration of the light emission spectrum:

$$k_r = \int_0^\infty \sigma_{em}(\omega)\, d\omega = k_r^{FC} + k_r^{FC/HT} + k_r^{HT} \quad (27)$$

where the three terms of $\sigma_{em}(\omega)$ are expressed in Appendix A (eqs A14−A16).

**B. Internal Conversion Rate.** According to Fermi's golden rule, the internal conversion (IC) rate can be presented as

$$k_{ic} = \frac{2\pi}{\hbar} |H'_{fi}|^2 \delta(E_{fi} + E_{fv_f} - E_{iv_i}) \quad (28)$$

Here the perturbation is the non-Born−Oppenheimer coupling

$$H'_{fi} = -\hbar^2 \sum_l \left\langle \Phi_f \Theta_{fv_f} \middle| \frac{\partial \Phi_i}{\partial Q_{fl}} \frac{\partial \Theta_{iv_i}}{\partial Q_{fl}} \right\rangle \quad (29)$$

Applying the Condon approximation, eq 29 becomes

$$H'_{fi} = \sum_l \langle \Phi_f | \hat{P}_{fl} | \Phi_i \rangle \langle \Theta_{fv_f} | \hat{P}_{fl} | \Theta_{iv_i} \rangle \quad (30)$$

Inserting (30) into (28), the IC rate can be expressed as[25]

$$k_{ic} = \sum_{kl} k_{ic,kl} \quad (31)$$

with

$$k_{ic,kl} = \frac{2\pi}{\hbar} R_{kl} Z_{iv}^{-1} \sum_{v_i,v_f} e^{-\beta E_{iv_i}} P_{kl} \delta(E_{fi} + E_{fv_f} - E_{iv_i}) \quad (32)$$

and

$$R_{kl} = \langle \Phi_f | \hat{P}_{fk} | \Phi_i \rangle \langle \Phi_i | \hat{P}_{fl} | \Phi_f \rangle \quad (33)$$

$$P_{kl} = \langle \Theta_{fv_f} | \hat{P}_{fk} | \Theta_{iv_i} \rangle \langle \Theta_{iv_i} | \hat{P}_{fl} | \Theta_{fv_f} \rangle \quad (34)$$

The delta function is again Fourier transformed as

$$k_{ic,kl} = \frac{1}{\hbar^2} R_{kl} \int_{-\infty}^\infty dt \, [e^{i\omega_{if}t} Z_{iv}^{-1} \rho_{ic,kl}(t,T)] \quad (35)$$

where $\rho_{ic,kl}(t,T)$ is the IC thermal vibration correlation function. The derived analytical expression is given in Appendix B.

**C. Electronic Part of the IC Rate.** The electronic coupling term of the IC rate of eq 35 can be carried out using wave function-based ab initio quantum chemistry approaches.[64] Alternative, time-dependent density functional theory (TDDFT) is an efficient way to calculate the coupling term approximately, which has attracted intensive interests recently.[65−74] Here, we first follow the wave function based approach and then give an electronic coupling formula based on the transition electric field, which is also applicable for TDDFT. Apply the following commutation relation,[19]

$$\left[\frac{\partial}{\partial Q_{fl}}, \hat{H}_{el}\right] = \frac{\partial \hat{V}}{\partial Q_{fl}} \quad (36)$$

where $\hat{H}_{el}$ is the electronic Hamiltonian, which excludes the kinetic energy operator of the nuclei and the spin−orbital coupling operator of electrons, and $\hat{V}(\mathbf{r},\mathbf{R})$ stands for the Coulomb interaction potential between electrons and nuclei. Noticing that $\hat{H}_{el}|\Phi_i^0\rangle = E(\Phi_i^0)|\Phi_i^0\rangle$ and $\hat{H}_{el}|\Phi_f^0\rangle = E(\Phi_f^0)|\Phi_f^0\rangle$, where $|\Phi_i^0\rangle$ and $|\Phi_f^0\rangle$ are the two electronic states at the equilibrium position of molecular structure in the ground state. $E(\Phi_i^0)$ and $E(\Phi_f^0)$ are the corresponding eigenenergies. Then we can obtain

$$\left\langle \Phi_f^0 \middle| \frac{\partial \hat{V}}{\partial Q_{fl}} \middle| \Phi_i^0 \right\rangle = [E(\Phi_i^0) - E(\Phi_f^0)] \left\langle \Phi_f^0 \middle| \frac{\partial}{\partial Q_{fl}} \middle| \Phi_i^0 \right\rangle \quad (37)$$

Expressing the electronic coupling term approximately by its value at the equilibrium position, we get

$$-i\hbar \left\langle \Phi_f \middle| \frac{\partial}{\partial Q_{fl}} \middle| \Phi_i \right\rangle \approx -i\hbar \frac{\langle \Phi_f^0 | \partial \hat{V}/\partial Q_{fl} | \Phi_i^0 \rangle}{E(\Phi_i^0) - E(\Phi_f^0)} \quad (38)$$

The potential $\hat{V}(\mathbf{r},\mathbf{R})$ depends on the position of electrons and nuclei, so

$$\frac{\partial \hat{V}}{\partial Q_{fk}} = -\sum_{\sigma,\alpha} \frac{\partial}{\partial Q_{fk}} \frac{Z_\sigma e^2}{|\mathbf{r}_\alpha - \mathbf{R}_\sigma|} =$$
$$\sum_{\sigma,\alpha} \sum_j \frac{1}{\sqrt{M_\sigma}} \frac{\partial q_{\sigma j}}{\partial Q_{fk}} \frac{Z_\sigma e^2 (r_{\alpha j} - R_{\sigma j})}{|\mathbf{r}_\alpha - \mathbf{R}_\sigma|^3}$$
$$= -\sum_\sigma \frac{Z_\sigma e^2}{\sqrt{M_\sigma}} \sum_j E_{\sigma j} L_{f\sigma j,k} \quad (39)$$

$\mathbf{r}_\alpha$ and $\mathbf{R}_\sigma$ are coordinates of the $\alpha$th electron and the $\sigma$th nucleus, respectively, and $j = x, y, z$ represents Cartesian

components. $Z_\sigma$ represents the number of the nuclear charge, and $M_\sigma$ represents the nuclear mass. $L_{f\sigma j,k} = \partial q_{\sigma j}/\partial Q_{fk}$ is a component of the $k$th eigenvector of the Hessian matrix. $E_{\sigma j} = \sum_\alpha e(r_{\sigma j} - R_{\sigma j})/|\mathbf{r}_\alpha - \mathbf{R}_\sigma|^3$ is the $j$th component of the electric field operator for the nucleus centered at $\sigma$. Then

$$\langle \Phi_f^0 | \partial V/\partial Q_{fk} | \Phi_i^0 \rangle = -\sum_\sigma \frac{Z_\sigma e^2}{\sqrt{M_\sigma}} \sum_j \langle \Phi_f^0 | E_{\sigma j} | \Phi_i^0 \rangle L_{f\sigma j,k}$$

$$\equiv -\sum_\sigma \frac{Z_\sigma e^2}{\sqrt{M_\sigma}} \sum_j E_{f\leftarrow i,\sigma j} L_{f\sigma j,k}$$

$$(40)$$

where

$$E_{f\leftarrow i,\sigma j} = \langle \Phi_f^0 | E_{\sigma j} | \Phi_i^0 \rangle = \int d\mathbf{r} \rho_{fi}^0(\mathbf{r}) \frac{e(r_{\alpha j} - R_{\sigma j})}{|\mathbf{r}_\alpha - \mathbf{R}_\sigma|^3}$$

$$(41)$$

$\rho_{fi}^0(\mathbf{r})$ is the electronic transition density at the equilibrium position. $E_{f\leftarrow i,\sigma j}$ is the $j$th component of the transition electric field at atomic center $\sigma$, which can be obtained directly from wave function-based ab initio quantum chemistry or TDDFT calculation.

The assumption in eq 37 is that $|\Phi_f^0\rangle$ and $|\Phi_i^0\rangle$ are the exact eigenstates of $\hat{H}_{el}$. This condition is generally not satisfied when finite, atom-centered basis sets are used and leads to additional Pulay terms that vanish in the complete basis-set limit, It should be noted that recently Send and Furche[65] derived an exact derivative coupling between time-dependent Kohn–Sham determinants in a finite atom-centered basis set, which largely improve the convergence for finite contracted basis sets, and will be considered in the future.

**D. Inclusion of Dephasing Effects.** If dephasing effects arising from the interactions with the environment are included, the $\delta$ function in eqs 10, 11, and 28 can be extended to either a Lorentzian function (homogeneous dephasing)

$$D(\omega',\omega,\sigma) \equiv \frac{1}{\pi} \frac{\gamma}{(\omega - \omega')^2 + \gamma^2} \quad (42)$$

or a Gaussian function (inhomogeneous dephasing)

$$D(\omega',\omega,\sigma) \equiv \frac{1}{\sigma\sqrt{2\pi}} \exp\{-(\omega - \omega')^2/2\sigma^2\} \quad (43)$$

Then the absorption, emission spectra, and internal conversion rate can be broadened in the frequency domain.

$$\bar{\sigma}_{abs}(\omega) = \int \sigma_{abs}(\omega') D(\omega',\omega,\sigma) \, d\omega' \quad (44)$$

$$\bar{\sigma}_{em}(\omega) = \int \sigma_{em}(\omega') D(\omega',\omega,\sigma) \, d\omega' \quad (45)$$

$$\bar{k}_{ic}(\omega_{if}) = \int k_{ic}(\omega') D(\omega',\omega_{if},\sigma) \, d\omega' \quad (46)$$

or equivalently, for correlation functions in time domain,

$$\bar{\rho}_{abs}(t,T) = \rho_{abs}(t,T)e^{-\gamma|t|} \quad \text{or} \quad \rho_{abs}(t,T)e^{-\sigma^2 t^2/2}$$

$$(47)$$

$$\bar{\rho}_{emi}(t,T) = \rho_{emi}(t,T)e^{-\gamma|t|} \quad \text{or} \quad \rho_{emi}(t,T)e^{-\sigma^2 t^2/2}$$

$$(48)$$

$$\bar{\rho}_{ic}(t,T) = \rho_{ic}(t,T)e^{-\gamma|t|} \quad \text{or} \quad \rho_{ic}(t,T)e^{-\sigma^2 t^2/2}$$

$$(49)$$

The dephasing term helps to converge the time integration of the correlation function in some cases, especially at low temperatures or when the vibronic coupling is small. But it should be much less than the intrinsic vibronic coupling induced line-width broadening.

## IV. Computational Details

Geometry optimization and frequency calculations were carried out with the TURBOMOLE 6.0 program package.[75,76] The geometry of the ground state was optimized with DFT.[77] For the excited state, TDDFT was applied. The EGRAD module, which provides TDDFT analytic energy gradients, was utilized.[78] The B3LYP functional[79,80] and SV(P) basis sets[81] from the TURBOMOLE library were used. In general, DFT calculations with the B3LYP hybrid functional overestimate the vibrational frequencies and so we follow the common practice of scaling the computed results by a factor 0.9614, according to Koch and Holsthausen.[82] The derivative of the transition dipole moments $\bar{\mu}_{fi}$ were calculated numerically around the equilibrium position of the ground state. The transition electric field appeared in eq 41 $E_{f\leftarrow i,\sigma j}$ for electronic coupling was obtained from TDDFT calculation in Gaussian 03 program package.[83–85] The correlation function of absorption, emission, and internal conversion were calculated with home-built programs. The Fourier transformation of the correlation functions were carried out with the FFT routines of the FFTW LIBRARY (version 3.1.2).[86]

## V. Applications

**A. Room Temperature Absorption and Fluorescence Spectra of Free-Base Porphyrin.** Porphyrin possesses a weakly dipole-allowed transition between the ground and excited states. We take it as the first example to test the validity of our formalism. Porphyrins play key roles in many important biological processes such as photosynthesis, electron transfer, and oxygen absorption and transport.[87] The electronic structure
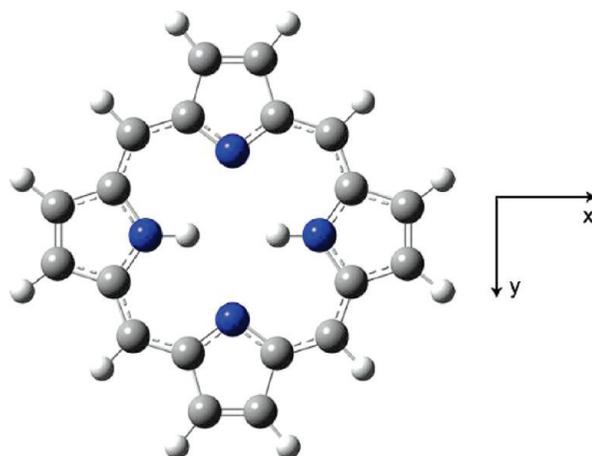


**Figure 1.** Structure of free-base porphyrin.

Feature Article

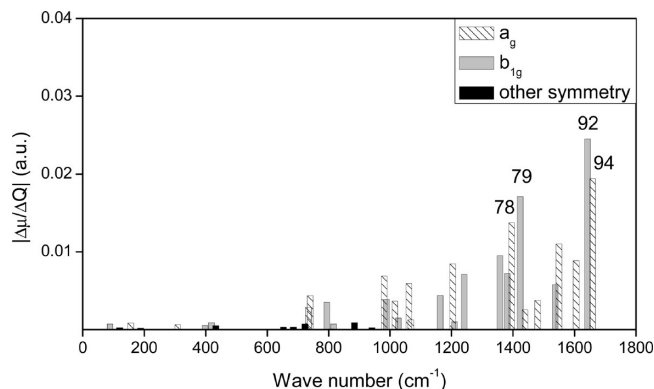*J. Phys. Chem. A, Vol. 114, No. 30, 2010* **7823**



**Figure 2.** Derivatives of the transition dipole moment with respect to the normal mode coordinates of porphyrin. The four components $\vec{\mu}_{78}$, $\vec{\mu}_{79}$, $\vec{\mu}_{92}$, and $\vec{\mu}_{94}$ reflect four normal modes that give large contributions to the Herzberg−Teller term.

and spectra of free-base porphyrin (H$_2$P) has been extensively investigated.[50,88−90] Edwards and co-workers performed the first extensive investigation on the spectroscopic properties of porphyrins in the vapor phase. The Q band (dark) and B band (intense, also called the Soret band) exist in the visible and near-UV region of the spectrum respectively and can be nicely interpreted within a four-orbital model proposed by Gouterman.[91,92] Unlike metal-porphyrin complexes which have $D_{4h}$ symmetry, H$_2$P belongs to the lower symmetry of $D_{2h}$. As a result, the degenerate Q band splits into Q$_x$ and Q$_y$ bands corresponding

to the two lowest weakly dipole-allowed electronic transitions. So the Herzberg−Teller effect dominates the Q band shape. Barone and co-workers have calculated the fluorescence and absorption spectra of H$_2$P including both DRE and HT effects using a sum-over-states method.[50] Here, we calculate the spectra applying our correlation function formalism for a comparison.

We used DFT (B3LYP/SV(P)) to optimize the geometry of the ground state S$_0$ and TDDFT (B3LYP/SV(P)) to optimize the geometry of the first excited state S$_1$. The transition dipole moment $\vec{\mu}_{fi}$ was found to be polarized along the $x$-axis, with magnitudes 0.0111 and 0.1156 au at the equilibrium geometry of S$_0$ and S$_1$, respectively. $\vec{\mu}_{fi}$ was then expanded around the minimum of $S_0$. The first derivatives of the electronic transition dipole moment with respect to the normal coordinates $\vec{\mu}_k \approx \Delta\vec{\mu}_{fi}/\Delta Q_k$ were obtained numerically and depicted in Figure 2. In our calculation, $\Delta Q_k$ is set to 0.01 au. $\vec{\mu}_k$ with symmetry a$_g$ are polarized along the $x$-axis and $\vec{\mu}_k$ with symmetry b$_{1g}$ are polarized along the $y$-axis. $\vec{\mu}_k$ with other symmetries contribute much less to the HT spectra. As seen in Figure 2, $\vec{\mu}_{78}$ (1395 cm$^{-1}$), $\vec{\mu}_{79}$ (1423 cm$^{-1}$), $\vec{\mu}_{92}$ (1642 cm$^{-1}$), and $\vec{\mu}_{94}$ (1659 cm$^{-1}$) are the four components that contribute most to the optical spectra.

These four modes cause relatively large modifications in transition density. According to eq 15, $\vec{\mu}_k$ is proportional to the space integration of the derivative of the transition density $\rho'_k$. To visualize the HT transition in real space, $\rho'_{78}$, $\rho'_{79}$, $\rho'_{92}$, and $\rho'_{94}$ are calculated and presented in Figure 3. The isovalues are set between $-2.0 \times 10^{-5}$ and $+2.0 \times 10^{-5}$ au. Vibrations with



(a). $\rho'_{78}\,(a_g)$

(b). $\rho'_{79}\,(b_{1g})$

(c). $\rho'_{92}\,(b_{1g})$
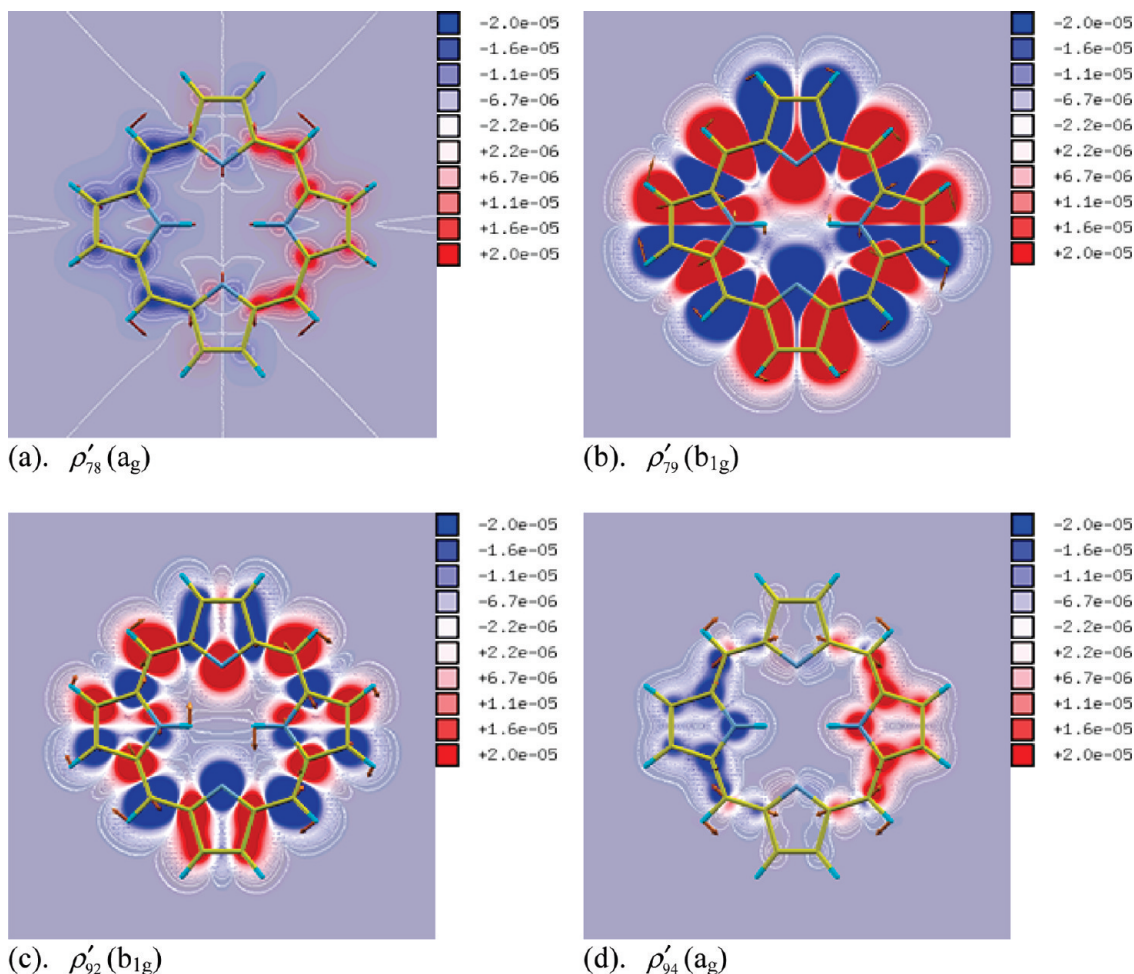
(d). $\rho'_{94}\,(a_g)$

**Figure 3.** Contour plots of derivatives of the transition density according to eq 15 in atomic units. (a)−(d) correspond to first derivatives of the dipole with respect to normal modes $Q_{78}$, $Q_{79}$, $Q_{92}$, and $Q_{94}$, respectively, which make the largest contributions to the Herzberg−Teller term.
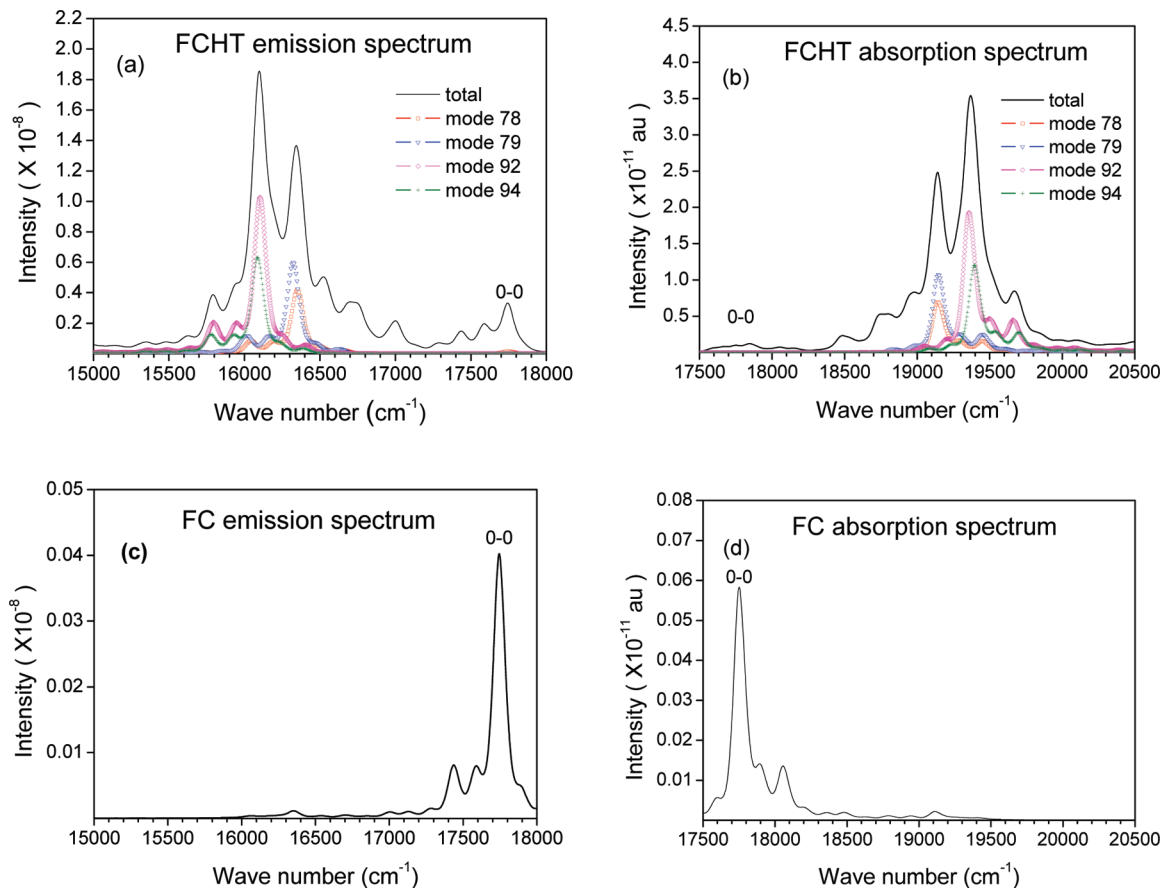
**Figure 4.** Calculated emission and absorption spectra of $H_2P$ at $T = 300$ K. (a) and (b) are emission and absorption spectra including both FC and HT contributions; (c) and (d) are emission and absorption spectra including only the FC contribution.

$a_g$ symmetry do not change the $D_{2h}$ symmetry of the molecule. As a result, $\vec{\mu}_{78}$ and $\vec{\mu}_{94}$ are polarized along the $x$-axis, which is the same as $\vec{\mu}_0$ at $S_0$. Vibration with $b_{1g}$ symmetry lifts the molecular symmetry from $D_{2h}$ to $C_{2h}$. $\vec{\mu}_{79}$ and $\vec{\mu}_{92}$ are then polarized along the $y$-axis. The absorption and emission spectra at 300 K are shown in Figure 4. The emission and absorption spectra are computed according to eqs A22 and A23 in atomic units. The total time interval is set to [−6553.6 fs, +6553.6 fs]. The time increment, $\Delta t$, is set to 0.1 fs. Since porphyrin is rigid, the difference in geometry between the ground state and the first excited state is small, with correspondingly small reorganization energies[35,93] of 160 cm$^{-1}$ (ground state) and 145 cm$^{-1}$ (first excited state). The FC spectrum is therefore narrowly centered around the 0−0 transition. The total FCHT spectra are calculated according to eqs A22 and A23, including FC, FC/HT, and HT contributions. The contribution of each single mode 78, 79, 92, and 94 to the FCHT spectra in Figure 4a,b was calculated according the corresponding FC/HT term in eq A19, and the diagonal element of HT term in eq A20. The calculated spectra are in good agreements with previous results.[50]

**B. Spectra and Emission Rate of Anthracene, Tetracene, and Pentacene.** Anthracene, tetracene, and pentacene are typical linear polyacenes. Their derivatives have important photophysical properties and have been widely investigated.[94−98] These linear polyacenes all belong to the $D_{2h}$ symmetry group. Their electronic and photophysical properties are correlated to the number of phenyl rings.[99] TDDFT calculations indicate that the lowest excited state $S_1$ is a dipole-allowed state with $B_{2u}$ symmetry, which is denoted as the $L_a$ state in Platt's nomenclature.[100] The FC term dominates the entire line shape of the absorption and emission spectra. In the calculation of the
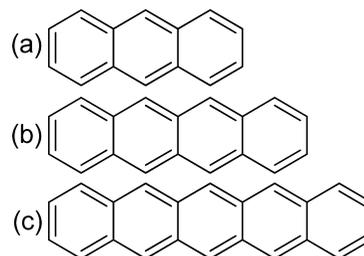


**Figure 5.** Molecular structures of anthracene (a), tetracene (b), and pentacene(c).

radiative rate, the HT correction accounts for about 10%. In this section, optical spectra including the HT term are calculated and compared to previous work. We also examine the dependence of the radiative decay rate on the number of phenyl rings with our formalism.

The experimental result shown in Figure 6 is for the anthracene vapor absorption spectrum at $T = 423$ K.[102] The experimental and calculated spectra are normalized to the signal of the highest intensity and the 0−0 transition energies ($\hbar\omega_{00}$) are set to zero. The result calculated in ref 101 is absorption spectrum at $T = 0$ K with a Gaussian broadening of fwhm = 330 cm$^{-1}$. The hot band transition located 300−750 cm$^{-1}$ below the 0−0 transition was missing there due to the omission of temperature effect. Within our formalism, the hot band found in measurements is fully recovered and found to be in good agreement with experiment. Figure 7 compares results of supersonic molecular beam spectroscopy[103] at $T$(nozzle) = 433 K with the calculated emission spectrum of anthracene. The entire spectral shape of the experiment, including the hot band,

Feature Article

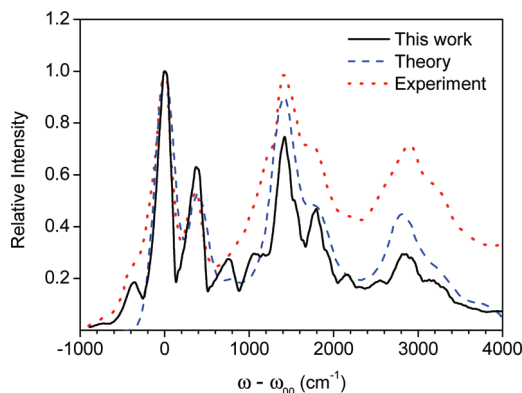*J. Phys. Chem. A, Vol. 114, No. 30, 2010* **7825**



**Figure 6.** Comparison of our calculated result (solid line) with previous theoretical calculation in ref 101 (dashed line) and with the experimental vapor absorption spectra in ref 102 (dotted line) at $T = 423$ K for the $1\ ^1A_g \rightarrow 1\ ^1B_{2u}\ (^1L_a)$ transition in anthracene.
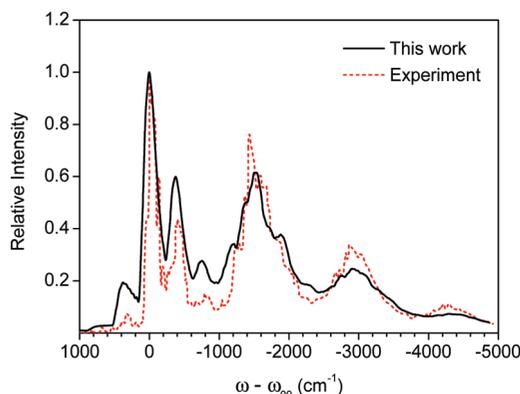


**Figure 7.** Comparison of our calculated emission spectrum (solid line) with supersonic molecular beam spectroscopy at $T = 433$ K in ref 103 (dashed line) for the $1\ ^1B_{2u}\ (^1L_a) \rightarrow 1\ ^1A_g$ transition in anthracene.
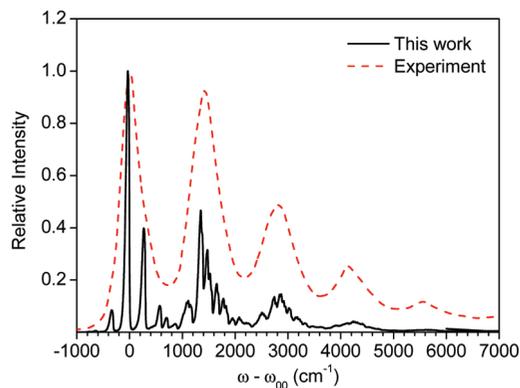


**Figure 8.** Comparison of our calculated result (solid line) and experimental absorption spectrum in ref 104 (dashed line) at $T = 300$ K for the $1\ ^1A_g \rightarrow 1\ ^1B_{2u}\ (^1L_a)$ transition in tetracene.

is well reproduced by our calculations without invoking any broadening factor.

The absorption and emission spectra of tetracene calculated at $T = 300$ K, including the HT term, are shown in Figures 8 and 9. It should be noted that although we find good correspondence between the experimental spectra and theory, the former is broader than the latter, most likely due to dephasing effects arising from interactions between the molecule and environment. Dephasing is also found to play an even more important effect in the calculations on azulene shown below.

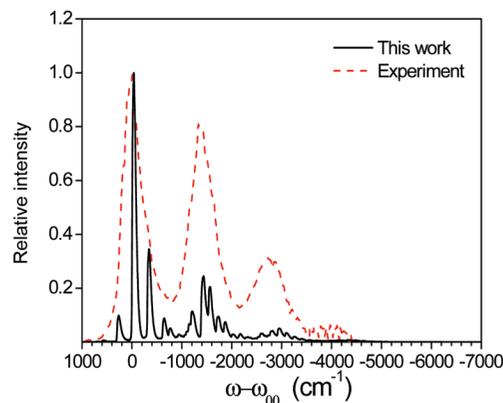For pentacene, high-resolution absorption and emission spectra have been measured in hexadecane matrices at 5 K.[105]



**Figure 9.** Comparison of our calculated result (solid line) and experimental emission spectrum in ref 104 (dashed line) at $T = 300$ K for the $1\ ^1B_{2u}\ (^1L_a) \rightarrow 1\ ^1A_g$ transition in tetracene.
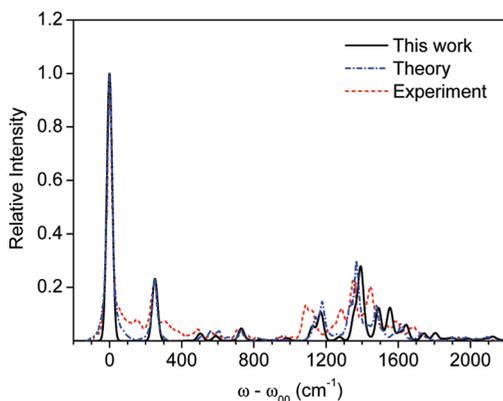


**Figure 10.** Comparison of our calculated result (solid line) with previous theoretical calculation in ref 101 (dashed line) and experimental absorption spectra in ref 105 (dotted line) at $T = 5$ K for the $1\ ^1A_g \rightarrow 1\ ^1B_{2u}\ (^1L_a)$ transition in pentacene. The Lorentzian broadening with fwhm = 30 cm$^{-1}$ has been applied.

Previous theoretical calculations of the absorption spectrum[101] included only the FC term and broadened via a Lorentzian with fwhm = 30 cm$^{-1}$. In our calculations, integration of the correlation function is found to diverge without inclusion of a dephasing factor, due to the extremely low temperature. Inclusion of a Lorentzian function with fwhm = 30 cm$^{-1}$ at $T = 5$ K led to the numerically converged spectra of Figures 10 and 11. We find that the peak at 1556 cm$^{-1}$ of absorption spectrum in Figure 10 is caused by the HT term, which was missing in the calculations of ref 101. The experimental spectra, including features with small intensity, are nicely reproduced by our calculations.

We next calculate the radiative decay rate for anthracene, tetracene, and pentacene at $T = 297$ K. Inclusion of the Herzberg−Teller effect is found to enhance the radiative decay rates by about 8−10% compared to the FC only approximation (see Table 1). According to eq 11, the radiative decay rate is directly proportional to $\omega^3$. Since the excitation energy (including zero point energy) $E^{0-0}$ decreases with the number of benzenes, so does the radiative decay rate.

**C. Radiative and Nonradiative Transition Rate of Azulene.** Azulene is the classic example of a molecule that violates Kasha's rule that photon emission (fluorescence or phosphorescence) occurs only from the lowest-energy excited electronic state of a molecule. In 1955, Beer and Longuet-Higgins[106] reported fairly strong $S_2 \rightarrow S_0$ fluorescence of azulene, whereas $S_1 \rightarrow S_0$ fluorescence and $T_1 \rightarrow S_0$ phosphorescence were too weak to be observed. These results were quickly confirmed by
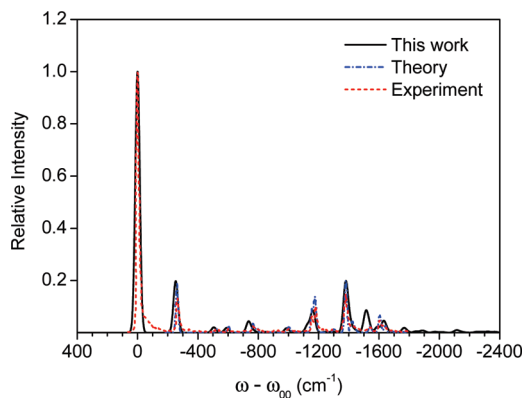
**7826** *J. Phys. Chem. A, Vol. 114, No. 30, 2010*

Niu et al.



**Figure 11.** Comparison of our calculated result (solid line) with previous theoretical calculation in ref 105 (dashed line) and experimental emission spectra in ref 105 (dotted line) at $T = 5$ K for the $1\ ^1B_{2u}\ (^1L_a) \rightarrow 1\ ^1A_g$ transition in pentacene. The Lorentzian broadening with fwhm $= 30\ cm^{-1}$ has been applied.

**TABLE 1: $E^{0-0}$ and Radiative Rates of Anthracene, Tetracene, and Pentacene**

| | this work | | | experiment (ref 99) | |
|---|---|---|---|---|---|
| | $E^{0-0}$ (eV) | $k_r$ (FC) ($s^{-1}$) | $k_r$ (FCHT) ($s^{-1}$) | $E^{0-0}$ (eV) | $k_r$ ($s^{-1}$) |
| anthracene | 2.94 | $2.28 \times 10^7$ | $2.51 \times 10^7$ | 3.30 | $6.20 \times 10^7$ |
| tetracene | 2.24 | $1.27 \times 10^7$ | $1.38 \times 10^7$ | 2.60 | $3.49 \times 10^7$ |
| pentacene | 1.73 | $0.73 \times 10^7$ | $0.81 \times 10^7$ | 2.11 | $1.20 \times 10^7$ |

Viswanath and Kasha.[107] Later Rentzepis observed very weak $S_1 \rightarrow S_0$ fluorescence and $T_1 \rightarrow S_0$ phosphorescence.[108,109] Hochstrasser and Ippen detected that the lifetime of $S_1$ is on the order of 2−4 ps.[110,111] Huppert also reported the quantum yields of $S_2 \rightarrow S_0$ (0.2), $S_2 \rightarrow S_1$ ($5 \times 10^{-4}$), and $S_1 \rightarrow S_0$ ($8 \times 10^{-6}$) emission in the vapor phase, which are approximately the same as those seen in solution.[112] The high-resolution absorption spectrum of the $S_0 \rightarrow S_1$ transition of jet-cooled azulene has been observed and the lifetime was estimated to be ~1 ps from the observed width of each vibronic band.[113,114] The strong $S_2 \rightarrow S_0$ fluorescence can be attributed to the relatively large $S_2 \rightarrow S_1$ energy gap, which slows down the $S_2 \rightarrow S_1$ internal conversion.[22] In addition, the relatively large $S_1 \rightarrow S_0$ internal conversion rate causes extremely weak $S_1 \rightarrow S_0$ fluorescence. Our goal is to quantitatively account for these observations using first-principles calculations.

We have performed TDDFT calculations for azulene. Optimization of the excited state $S_1$ yields $E^{0-0}$ (0−0 transition energy from $S_1$ to $S_0$) of 1.98 eV, which is a little larger than the experimental value of 1.78 eV in solution.[115] As shown in Figure 12, the excitation to the first excited state results in shortening of the inner C−C bond by more than 0.1 Å. In Figure 13, the calculated absorption spectrum shows excellent agreement with the low-resolution experimental spectrum,[115] which confirms the reliability of our DFT calculations.

The Duschinsky rotation matrix is presented in Figure 14. The geometries of the ground and excited states of azulene have the same symmetry ($C_{2v}$). The irreducible representations of the normal modes are classified into four irreducible representations, $17a_1 + 6a_2 + 9b_1 + 16b_2$. The vibrational modes of the two electronic states mix only within each irreducible block and are orthogonal between different blocks.

For the IC process of $S_1 \rightarrow S_0$ in azulene, the largest contribution comes from the diagonal terms $k_{ic,ll}$ (see eq 35). Recall that the electronic coupling prefactor for the IC rate is $R_{ll}/\hbar = |\langle\Phi_f|\hat{P}_{fl}|\Phi_i\rangle|^2/\hbar$. The irreducible representations of the
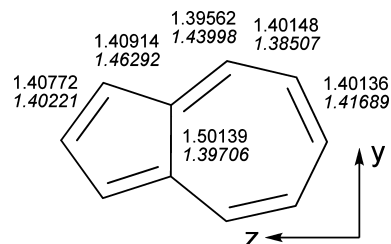


**Figure 12.** DFT optimized azulene structure. Bond lengths are indicated for the ground state and the first excited state (in italics).
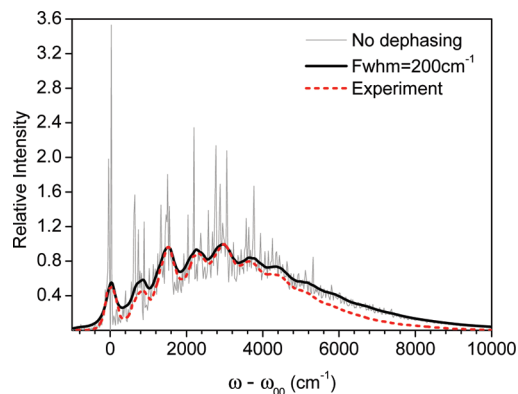


**Figure 13.** Comparison of our calculated result with experimental absorption spectrum in ref 115 at $T = 300$ K for the $1\ ^1A_1 \rightarrow 1\ ^1B_2$ transition in azulene. The thin and thick lines correspond to the calculated spectrum without and with dephasing, respectively. The dashed line is the experimental absorption spectrum of azulene in cyclohexane.
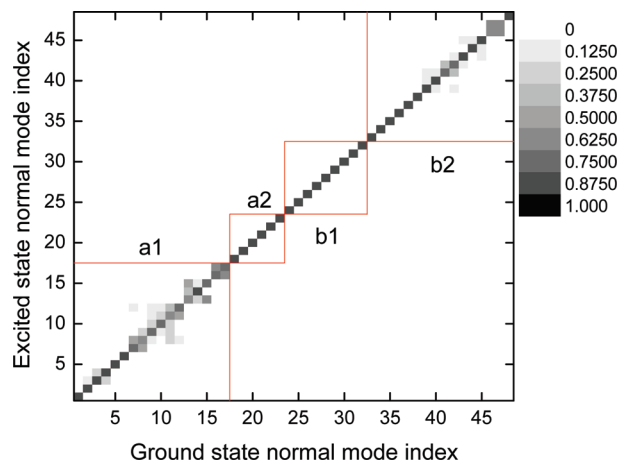


**Figure 14.** Duschinsky rotation matrix of azulene between the ground state and excited state normal modes, which is decomposed into four irreducible representations. The order of normal modes in the excited state is rearranged to make the largest element be the diagonal.

ground and excited electronic states are $a_1$ and $b_2$, respectively. Due to the transition selection rule, the nonzero $R_{ll}$ must come from normal modes with $b_2$ symmetry. Numerical calculations, according to eq 38, can give $R_{ll}$ from each normal mode $l$ and these are depicted in Figure 15.

The diagonal terms for the IC rate, $k_{ic,ll}$ of eq 35, are plotted in Figure 16. It is found that modes that make large contributions to $k_{ic}$ concentrate around 1000−1400 $cm^{-1}$. Since we do not assume a promoting mode, the total IC rate consists of both diagonal and off-diagonal contributions, and the numerical calculations include mode mixing effects through $R_{kl}$ and $\rho_{kl}$. The contribution from the sum of diagonal terms amounts to about 96% of the total.
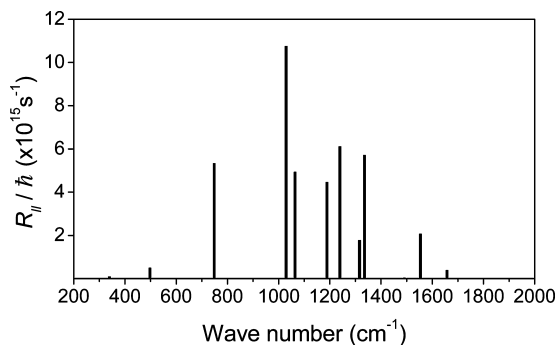
Feature Article

*J. Phys. Chem. A, Vol. 114, No. 30, 2010* **7827**



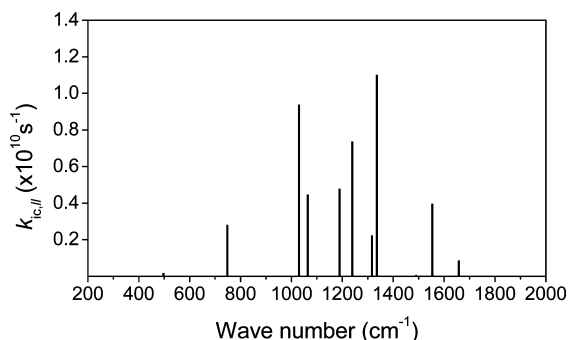**Figure 15.** Electronic coupling factors for the IC rate in azulene, $R_{ll}/\hbar$.



**Figure 16.** Diagonal matrix elements, $k_{ic,ll}$ of eq 35, for the IC rate in azulene.

**TABLE 2: Radiative Decay Rate and Internal Conversion Rate from $S_1 \rightarrow S_0$ of Azulene**

| | experiment[116] | | this work | |
|---|---|---|---|---|
| | $k_r$ (s$^{-1}$) | $k_{ic}$ (s$^{-1}$) | $k_r$ (s$^{-1}$) | $k_{ic}$ (s$^{-1}$) |
| $S_1$–$S_0$ | $1.0 \times 10^6$ | $5.0 \times 10^{11}$ | $1.12 \times 10^6$ | $0.23 \times 10^{11}$ |

The radiative decay rate and IC rate at $T = 300$ K are listed in Table 2. A Lorentzian broadening of 67 cm$^{-1}$ is applied to ensure convergence of the numerical integration for the correlation function. The total time interval for the correlation function is set to [−6553.6 fs, +6553.6 fs], with a time increment, $\Delta t$, of 0.001 fs. The IC rate $k_{ic}$ is calculated to be about 4 orders of magnitude larger than the radiative decay rate $k_r$, which approximately agrees with experiment. Furthermore, we find that the DRE enhances the IC rate of azulene. If we omit the Duschinsky mixing effect, the IC rate is calculated to be $0.04 \times 10^{11}$ s$^{-1}$, which amounts to only 17.4% of $k_{ic}$ with DRE. Such effect can be well understood from the plot of $\log(k_{ic})$ vs adiabatic energy gap in Figure 17.

The IC rate is dependent on the energy difference between two electronic states. Let us look at the IC rate as a function of the energy difference $\Delta E$, denoting the actual adiabatic transition energy of the molecule as $E_{ad}$. The actual IC rate is $k_{ic} = k_{ic}(E_{ad})$. This is quite similar to the generating function analysis,[117] for which $k_{ic} = k_{ic}(0) = (2\pi/\hbar)C^2 F(0)$. Here, $C^2$ is the electronic coupling term. $F(E)$, the line shape function, is the inverse Fourier transform of the generating function in ref 117. The generating function is just similar to the correlation function appeared in eq 21. Figure 17 shows the IC spectrum ($S_1 \rightarrow S_0$) with and without DRE. The adiabatic energy $E_{ad}$ is 16 324 cm$^{-1}$. The broadening effect from DRE enhances $k_{ic}$ for $\Delta E > 6200$ cm$^{-1}$, so the $k(E_{ad})$ increases due to DRE. The IC spectrum in Figure 17 follows the energy gap law.[117−120] When $\Delta E$ is large enough, $\log(k_{ic})$ decreases approximately linearly with $\Delta E$, or equivalently, $k_{ic}$ decreases exponentially with $\Delta E$. This result
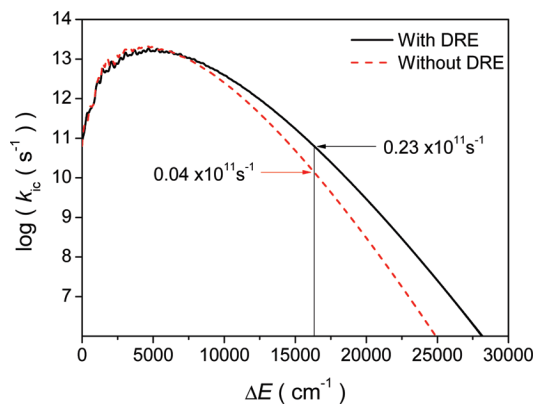


**Figure 17.** Internal conversion rate vs energy difference $\Delta E$ in azulene. The adiabatic energy $E_{ad} = 16324$ cm$^{-1}$. The solid line is the IC spectrum with DRE, which gives IC rate $= 0.23 \times 10^{11}$ s$^{-1}$, at $\Delta E = E_{ad}$. The dashed line is the IC spectrum without DRE, which gives IC rate $= 0.04 \times 10^{11}$ s$^{-1}$, at $\Delta E = E_{ad}$.

is in agreement with the energy gap law for nonradiative transitions in the weak coupling limit.[117,121,122] The total Huang−Rhys factor of azulene is about 2.786, which is larger than 1. If we apply a displaced oscillator model and short time approximation to the integration in eq 35 for one specific promoting mode, the rate can be expressed as

$$\log k_{ic,l}(\omega_{if}) \propto -(-\omega_{if} + \omega_l + \sum_{j(\neq l)} S_j\omega_j)^2/2 \sum_{j(\neq l)} S_j\omega_j^2(2\bar{n}_j + 1) \quad (50)$$

The maximum of $\log k_{ic,l}$ is at $E_{if} = \hbar\omega_l + \sum_{j(\neq l)}\lambda_j$, where $S_j = \omega_j D_j^2/2\hbar$ is the Huang−Rhys factor, and $D_j$ is the displacement of the $j$th mode. $\bar{n}_j = (\exp(\beta\hbar\omega_j) - 1)^{-1}$ is the phonon distribution function, and $\lambda_j = S_j\hbar\omega_j$ is the reorganization energy of the $j$th accepting mode. The largest contribution to the IC rate comes from the 32nd promoting mode 1335 cm$^{-1}$; see Figure 16. The reorganization energy is calculated to be 3253 cm$^{-1}$ and comes from $a_1$ symmetry accepting modes. So $\log k_{ic,32}$ peaks at 4588 cm$^{-1}$. This corresponds approximately to the peak in Figure 17. This is a typical Marcus theory behavior for the nonradiative decay process.

To summarize this part, we have demonstrated that the calculated optical absorption spectrum radiative and IC rate for azulene is in good agreement with the experiment, which further confirms the reliability of the present thermal vibration correlation function formalism. These results show the importance of DRE to enhance the IC rate in this case, and provide a proper explanation that the decay rate from $S_1$ to $S_0$ is dominated by IC. Besides, the line shape of IC rate with respects to adiabatic energy gap $\Delta E$ is shown to follow a linear energy gap law when $\Delta E$ is much larger than the reorganization energy and to follow Marcus theory behavior when $\Delta E$ is smaller.

## VI. Conclusion

In this paper, we have presented a general formalism to calculate optical absorption and emission spectra, along with the radiative and nonradiative decay rate constants, between two adiabatic electronic states, based on a thermal vibration correlation function formalism within a multidimensional harmonic oscillator model. The Duschinsky rotation effect and Herzberg−Teller effect are both included in the formalism. In contrast to the sum-over-states methods, the correlation function formalism can

automatically include all the transitions between the vibrational states of the two electronic states. This is important for calculations of the spectra and rate constants of large molecules, in which the DRE is significant, especially for the low frequency modes.[24] In fact, for polyatomic molecules, it is usually impossible to identify one or a few "important" vibrational modes. The present formalism allows inclusion of all the mode-mixing effects in the vibration correlation function part and all the modes in electronic couplings and mixings for nonradiative decay rate; i.e., the method is free of the promoting mode approximation.

We then applied the formalism to calculate the spectra of free-base porphyrin, anthracene, tetracene, pentacene, and azulene. The results show good agreement with the experiment counterparts. In the case of azulene, the internal conversion rate is calculated to be 4 orders of magnitude larger than the radiative decay rate for the $S_1 \rightarrow S_0$ transition. The internal conversion process was calculated to follow Marcus theory and was found to be largely enhanced by the Duschinsky rotation effect. It should be pointed out that at present, we have not considered the anharmonicity, which would certainly be important for the excited state processes. For polyatomic molecules, it is impossible to consider the actual potential energy surfaces for both ground and excited states. In this regard, we note that recent progresses on "dynamics on-the-fly"[123,124] holds some promise. Alternatively, within the correlation function formalism, it is possible to including anharmonicity perturbatively by expanding the PES to the cubic and quartic terms.[125] Both of these are in active progress now in our group.

**Appendix A: Analytical Formulas for Optical Emission and Absorption Spectra.**

The Franck−Condon correlation function can be evaluated analytically:

$$\rho_{em,0}^{FC}(t,T) = Tr[e^{-i\tau_f \hat{H}_f} e^{-i\tau_i \hat{H}_i}]$$

$$= \sqrt{\frac{\det[\mathbf{a_f a_i}]}{\det[\mathbf{B}] \det[\mathbf{B} - \mathbf{A B}^{-1}\mathbf{A}]}}$$
$$\exp\left\{\frac{i}{\hbar}[\underline{D}^T \mathbf{ES}(\mathbf{B} - \mathbf{A})^{-1}\mathbf{GS}^T \underline{D}]\right\} \tag{A1}$$

where **A**, **B**, **G**, and **E** are defined as

$$\mathbf{A} = \mathbf{a_f} + \mathbf{S}^T \mathbf{a_i S} \tag{A2}$$

$$\mathbf{B} = \mathbf{b_f} + \mathbf{S}^T \mathbf{b_i S} \tag{A3}$$

$$\mathbf{G} = \mathbf{b_f} - \mathbf{a_f} \tag{A4}$$

$$\mathbf{E} = \mathbf{b_i} - \mathbf{a_i} \tag{A5}$$

Here, $\mathbf{a_{i,f}}$ and $\mathbf{b_{i,f}}$ are diagonal matrices with diagonal elements $a_{i,fk}(\tau) = \omega_{i,fk}/\sin(\hbar\omega_{i,fk}\tau_{i,f})$, and $b_{i,fk}(\tau) = \omega_{i,fk}/\tan(\hbar\omega_{i,fk}\tau_{i,f})$ for the initial and final electronic states respectively.

To get a unified form for eqs 24, 25, and 26, we define two matrices

$$\mathbf{K} = \begin{bmatrix} \mathbf{B} & -\mathbf{A} \\ -\mathbf{A} & \mathbf{B} \end{bmatrix}_{2N \times 2N} \tag{A6}$$

$$\underline{F} = [\underline{D}^T \mathbf{ES} \quad \underline{D}^T \mathbf{ES}]_{1 \times 2N}^T \tag{A7}$$

Then (A1) can be recast as

$$\rho_{em,0}^{FC}(t,T) = \sqrt{\frac{\det[\mathbf{a_f a_i}]}{\det[\mathbf{K}]}} \exp\left\{-\frac{i}{\hbar}\left[\frac{1}{2}\underline{F}^T \mathbf{K}\underline{F} - \underline{D}^T \mathbf{ED}\right]\right\} \tag{A8}$$

For the FCHT spectrum, we need to define an auxiliary column matrix,

$$\underline{H}_k^{FC/HT} = [0_1 \cdots 1_k \cdots 0_{2N}]_{1 \times 2N}^T \tag{A9}$$

Then eq 25 becomes

$$\rho_{em,k}^{FC/HT}(t,T) = -\rho_{em,0}^{FC}(t,T)\{(\underline{H}_k^{FC/HT})^T \mathbf{K}^{-1}\underline{F}\} \tag{A10}$$

For the HT spectrum, we define a square matrix,

$$\mathbf{G}_{kl}^{HT} = \begin{bmatrix} 0_{11} & 0_{12} & \cdots & 0_{1N+l} & \cdots \\ 0_{21} & 0_{22} & \cdots & 0_{2N+l} & \cdots \\ \cdots & \cdots & \cdots & \cdots & \cdots \\ 0_{k1} & 0_{k2} & \cdots & 1_{kN+l} & \cdots \\ \cdots & \cdots & \cdots & \cdots & \cdots \end{bmatrix} \tag{A11}$$

Then the HT term, eq 26, becomes

$$\rho_{em,kl}^{HT}(t,T) = \rho_{em,0}^{FC}(t,T)\{i\hbar Tr[\mathbf{G}_{kl}^{HT}\mathbf{K}^{-1}] + (\mathbf{K}^{-1}\underline{F})^T \mathbf{G}_{kl}^{HT}(\mathbf{K}^{-1}\underline{F})\} \tag{A12}$$

The emission spectrum then becomes

$$\sigma_{em}(\omega) = \sigma_{em}^{FC}(\omega) + \sum_k \sigma_{em,k}^{FC/HT}(\omega) + \sum_{k,l} \sigma_{em,kl}^{HT}(\omega) \tag{A13}$$

where

Feature Article

*J. Phys. Chem. A, Vol. 114, No. 30, 2010* **7829**

$$\sigma_{\text{em}}^{\text{FC}}(\omega) = \frac{2\omega^3}{3\pi\hbar c^3}|\vec{\mu}_0|^2 \int e^{-i(\omega-\omega_{if})t} Z_{i\nu}^{-1} \rho_{\text{em},0}^{\text{FC}}(t,T)\,dt \tag{A14}$$

$$\sigma_{\text{em},k}^{\text{FC/HT}}(\omega) = \frac{2\omega^3}{3\pi\hbar c^3}\vec{\mu}_0\cdot\vec{\mu}_k \int e^{-i(\omega-\omega_{if})t} Z_{i\nu}^{-1} \rho_{\text{em},k}^{\text{FC/HT}}(t,T)\,dt \tag{A15}$$

$$\sigma_{\text{em},kl}^{\text{HT}}(\omega) = \frac{2\omega^3}{3\pi\hbar c^3}\vec{\mu}_k\cdot\vec{\mu}_l \int e^{-i(\omega-\omega_{if})t} Z_{i\nu}^{-1} \rho_{\text{em},kl}^{\text{HT}}(t,T)\,dt \tag{A16}$$

The absorption spectrum possesses a form very similar to that of the emission spectrum,

$$\sigma_{\text{abs}}(\omega) = \sigma_{\text{abs}}^{\text{FC}}(\omega) + \sum_k \sigma_{\text{abs},k}^{\text{FC/HT}}(\omega) + \sum_{k,l} \sigma_{\text{abs},kl}^{\text{HT}}(\omega) \tag{A17}$$

where

$$\sigma_{\text{abs}}^{\text{FC}}(\omega) = \frac{2\pi\omega}{3\hbar c}|\vec{\mu}_0|^2 \int e^{i(\omega-\omega_{fi})t} Z_{i\nu}^{-1} \rho_{\text{abs},0}^{\text{FC}}(t,T)\,dt \tag{A18}$$

$$\sigma_{\text{abs},k}^{\text{FC/HT}}(\omega) = \frac{2\pi\omega}{3\hbar c}\vec{\mu}_0\cdot\vec{\mu}_k \int e^{i(\omega-\omega_{fi})t} Z_{i\nu}^{-1} \rho_{\text{abs},k}^{\text{FC/HT}}(t,T)\,dt \tag{A19}$$

$$\sigma_{\text{abs},kl}^{\text{HT}}(\omega) = \frac{2\pi\omega}{3\hbar c}\vec{\mu}_k\cdot\vec{\mu}_l \int e^{i(\omega-\omega_{fi})t} Z_{i\nu}^{-1} \rho_{\text{abs},kl}^{\text{HT}}(t,T)\,dt \tag{A20}$$

Defining

$$\tilde{\mu}_{\text{em}}^2(t,T) = |\vec{\mu}_0|^2 - \sum_k \vec{\mu}_0\cdot\vec{\mu}_k[(\underline{H}_k^{\text{FC/HT}})^{\text{T}}\mathbf{K}^{-1}\underline{F}] +$$
$$\sum_{kl} \vec{\mu}_k\cdot\vec{\mu}_l[i\hbar\text{Tr}[\mathbf{G}_{kl}^{\text{HT}}\mathbf{K}^{-1}] + (\mathbf{K}^{-1}\underline{F})^{\text{T}}\mathbf{G}_{kl}^{\text{HT}}(\mathbf{K}^{-1}\underline{F})] \tag{A21}$$

the emission spectrum becomes

$$\sigma_{\text{em}}(\omega) = \frac{2\omega^3}{3\pi\hbar c^3} \int e^{-i(\omega-\omega_{if})t} Z_{i\nu}^{-1} \rho_{\text{em},0}^{\text{FC}}(t,T)\,\tilde{\mu}_{\text{em}}^2(t,T)\,dt \tag{A22}$$

and the final form of absorption spectrum is

$$\sigma_{\text{abs}}(\omega) = \frac{2\pi\omega}{3\hbar c} \int e^{i(\omega-\omega_{fi})t} Z_{i\nu}^{-1} \rho_{\text{abs},0}^{\text{FC}}(t,T)\,\tilde{\mu}_{\text{abs}}^2(t,T)\,dt \tag{A23}$$

## Appendix B: Analytical Formulas for Internal Conversion Rate.

The internal conversion thermal vibration correlation function is

$$\rho_{\text{ic},kl}(t,T) = \text{Tr}[\hat{P}_{fk}e^{-i\tau_f\hat{H}_f}\hat{P}_{fl}e^{-i\tau_i\hat{H}_i}] \tag{B1}$$

The final form after continuously inserting complete set and carrying Gaussion integrations is expressed as (see ref 25):

$$\rho_{\text{ic},kl}(t,T) = \sqrt{\frac{\det[\mathbf{a}_f\mathbf{a}_i]}{\det[\mathbf{K}]}}\exp\left\{-\frac{i}{\hbar}\left[\frac{1}{2}\underline{F}^{\text{T}}\mathbf{K}^{-1}\underline{F} - \underline{D}^{\text{T}}\mathbf{E}\underline{D}\right]\right\}\cdot\{i\hbar\text{Tr}[\mathbf{G}_{kl}^{\text{IC}}\mathbf{K}^{-1}] + (\mathbf{K}^{-1}\underline{F})^{\text{T}}\mathbf{G}_{kl}^{\text{IC}}(\mathbf{K}^{-1}\underline{F}) - (\underline{H}_{kl}^{\text{IC}})^{\text{T}}\mathbf{K}^{-1}\underline{F}\} \tag{B2}$$

where

$$\mathbf{G}_{kl}^{\text{IC}} = \begin{bmatrix} \mathbf{G}_{kl,11}^{\text{IC}} & \mathbf{G}_{kl,12}^{\text{IC}} \\ \mathbf{G}_{kl,21}^{\text{IC}} & \mathbf{G}_{kl,22}^{\text{IC}} \end{bmatrix} \tag{B3}$$

$$\mathbf{G}_{kl,11}^{\text{IC}} = \begin{bmatrix} \dots \\ 0 \\ -b_{fk}[\mathbf{S}^{\text{T}}\mathbf{a}_i\mathbf{S}]_{l\to k} \\ 0 \\ \dots \end{bmatrix} \tag{B4}$$

$$\mathbf{G}_{kl,12}^{\text{IC}} = \begin{bmatrix} \dots \\ 0 \\ b_{fk}[\mathbf{S}^{\text{T}}\mathbf{b}_i\mathbf{S}]_{l\to k} \\ 0 \\ \dots \end{bmatrix} \tag{B5}$$

$$\mathbf{G}_{kl,21}^{\text{IC}} = \begin{bmatrix} \dots \\ 0 \\ a_{fk}[\mathbf{S}^{\text{T}}\mathbf{a}_i\mathbf{S}]_{l\to k} \\ 0 \\ \dots \end{bmatrix} \tag{B6}$$

$$\mathbf{G}_{kl,22}^{\text{IC}} = \begin{bmatrix} \dots \\ 0 \\ -a_{fk}[\mathbf{S}^{\text{T}}\mathbf{b}_i\mathbf{S}]_{l\to k} \\ 0 \\ \dots \end{bmatrix} \tag{B7}$$

$$\underline{H}_{kl}^{\text{IC}} = \begin{bmatrix} \underline{H}_{kl,1}^{\text{IC}} \\ \underline{H}_{kl,2}^{\text{IC}} \end{bmatrix} \tag{B8}$$

$$\underline{H}_{kl,1}^{\text{IC}} = [\cdots\ 0\ b_{fk}[\underline{D}^{\text{T}}\mathbf{ES}]_{l\to k}\ 0\ \cdots]^{\text{T}} \tag{B9}$$

$$\underline{H}_{kl,2}^{\text{IC}} = [\cdots\ 0\ -a_{fk}[\underline{D}^{\text{T}}\mathbf{ES}]_{l\to k}\ 0\ \cdots]^{\text{T}} \tag{B10}$$

$[\mathbf{S}^{\text{T}}\mathbf{a}_i\mathbf{S}]_{l\to k}$ is the $l$th row of matrix $[\mathbf{S}^{\text{T}}\mathbf{a}_i\mathbf{S}]$, which is multiplied by $-b_{fk}$ and inserted into the $k$th row of $\mathbf{G}_{kl,11}^{\text{IC}}$. The remaining rows of $\mathbf{G}_{kl,11}^{\text{IC}}$ are null. $[\underline{D}^{\text{T}}\mathbf{ES}]_{l\to k}$ is the $l$th element of the row matrix $[\underline{D}^{\text{T}}\mathbf{ES}]$, which is multiplied by $b_{fk}$ and inserted into the $k$th row of $\underline{H}_{kl,1}^{\text{IC}}$. The remaining elements of $\underline{H}_{kl,1}^{\text{IC}}$ are null.

**7830** *J. Phys. Chem. A, Vol. 114, No. 30, 2010*

Niu et al.

## References and Notes

(1) Kimel, S.; Speiser, S. *Chem. Rev.* **1977**, *77*, 437.

(2) Wang, C. H. *Spectroscopy of Condensed Media: Dynamics of Molecular Interactions*; Academic Press: New York, 1985.

(3) Fleming, G. R. *Chemical Applications of Ultrafast Spectroscopy*; Oxford University Press: New York, 1986.

(4) Speiser, S. *Chem. Rev.* **1996**, *96*, 1953.

(5) Tang, C. W.; VanSlyke, S. A. *Appl. Phys. Lett.* **1987**, *51*, 913.

(6) Burroughes, J. H.; Bradley, D. D. C.; Brown, A. R.; Marks, R. N.; Mackay, K.; Friend, R. H.; Burns, P. L.; Holmes, A. B. *Nature* **1990**, *347*, 539.

(7) Gustafsson, G.; Cao, Y.; Treacy, G. M.; Klavetter, F.; Colaneri, N.; Heeger, A. J. *Nature* **1992**, *357*, 477.

(8) De Angelis, F.; Santoro, F.; Nazeruddin, M. K.; Barone, V. *J. Phys. Chem. B* **2008**, *112*, 13181.

(9) Tang, B. Z.; Zhan, X.; Yu, G.; Lee, P. P. S.; Liu, Y.; Zhu, D. *J. Mater. Chem.* **2001**, *11*, 2974.

(10) An, B.; Kwon, S.; Jung, S.; Park, S. Y. *J. Am. Chem. Soc.* **2002**, *124*, 14410.

(11) Chen, J.; Law, C. C. W.; Lam, J. W. Y.; Dong, Y.; Lo, S. M. F.; Williams, I. D.; Zhu, D.; Tang, B. Z. *Chem. Mater.* **2003**, *15*, 1535.

(12) An, B.; Lee, D.; Lee, J.; Park, Y.; Song, H.; Park, S. Y. *J. Am. Chem. Soc.* **2004**, *126*, 10232.

(13) Han, M.; Hara, M. *J. Am. Chem. Soc.* **2005**, *127*, 10951.

(14) Wang, F.; Han, M.; Mya, K. Y.; Wang, Y.; Lai, Y. *J. Am. Chem. Soc.* **2005**, *127*, 10350.

(15) Lee, S. H.; Jang, B.; Kafafi, Z. H. *J. Am. Chem. Soc.* **2005**, *127*, 9071.

(16) Tong, H.; Hong, Y.; Dong, Y.; Häussler, M.; Lam, J. W. Y.; Li, Z.; Guo, Z.; Guo, Z.; Tang, B. Z. *Chem. Commun.* **2006**, 3705.

(17) Tong, H.; Dong, Y.; Häußler, M.; Hong, Y.; Lam, J. W. Y.; Sung, H. H.; Williams, I. D.; Kwok, H. S.; Tang, B. Z. *Chem. Phys. Lett.* **2006**, *428*, 326.

(18) Zeng, Q.; Li, Z.; Dong, Y.; Di, C. A.; Qin, A.; Hong, Y.; Ji, L.; Zhu, Z.; Jim, C. K. W.; Yu, G.; Li, Q.; Li, Z.; Liu, Y.; Qin, J.; Tang, B. Z. *Chem. Commun.* **2007**, 70.

(19) Hayashi, M.; Mebel, A. M.; Liang, K. K.; Lin, S. H. *J. Chem. Phys.* **1998**, *108*, 2044.

(20) Mebel, A. M.; Hayashi, M.; Liang, K. K.; Lin, S. H. *J. Phys. Chem. A* **1999**, *103*, 10674.

(21) Yin, S.; Peng, Q.; Shuai, Z.; Fang, W.; Wang, Y.; Luo, Y. *Phys. Rev. B* **2006**, *73*, 205409.

(22) Islampour, R.; Miralinaghi, M. *J. Phys. Chem. A* **2007**, *111*, 9454.

(23) Peng, Q.; Yi, Y.; Shuai, Z.; Shao, J. *J. Chem. Phys.* **2007**, *126*, 114302.

(24) Peng, Q.; Yi, Y.; Shuai, Z.; Shao, J. *J. Am. Chem. Soc.* **2007**, *129*, 9333.

(25) Niu, Y.; Peng, Q.; Shuai, Z. *Sci. China Ser. B-Chem.* **2008**, *51*, 1153.

(26) Islampour, R.; Miralinaghi, M. *J. Phys. Chem. A* **2009**, *113*, 2340.

(27) Peng, Q.; Niu, Y.; Deng, C.; Shuai, Z. *Chem. Phys.* **2010**, *370*, 215.

(28) Peng, Q.; Niu, Y.; Shuai, Z. *Chem. J. Chin. Univ.* **2008**, *29*, 2435.

(29) Markham, J. J. *Rev. Mod. Phys.* **1959**, *31*, 956.

(30) Domcke, W.; Yarkony, D. R.; Koppel, H. *Conical Intersections*; World Scientific Publishing Company: Singapore, 2004.

(31) Duschinsky, F. *Acta Physicochim. (USSR)* **1937**, *7*, 551.

(32) Marcus, R. A. *J. Chem. Phys.* **1956**, *24*, 966.

(33) Marcus, R. A. *J. Chem. Phys.* **1956**, *24*, 979.

(34) Marcus, R. A. *Annu. Rev. Phys. Chem.* **1964**, *15*, 155.

(35) Lin, S. H.; Chang, C. H.; Liang, K. K.; Chang, R.; Shiu, Y. J.; Zhang, J. M.; Yang, T. S.; Hayashi, M.; Hsu, F. C. *Adv. Chem. Phys.* **2002**, *121*, 1.

(36) Book, L. D.; Arnett, D. C.; Hu, H.; Scherer, N. F. *J. Phys. Chem. A* **1998**, *102*, 4350.

(37) Sinclair, W. E.; Yu, H.; Phillips, D.; Hollas, J. M. *J. Chem. Phys.* **1997**, *106*, 5797.

(38) Eiden, G. C.; Weisshaar, J. C. *J. Chem. Phys.* **1996**, *104*, 8896.

(39) Falchi, A.; Gellini, C.; Salvi, P. R.; Hafner, K. *J. Phys. Chem.* **1995**, *99*, 14659.

(40) Lunardi, G.; Pecile, C. *J. Chem. Phys.* **1991**, *95*, 6911.

(41) Hemley, R. J.; Leopold, D. G.; Vaida, V.; Karplus, M. *J. Chem. Phys.* **1985**, *82*, 5379.

(42) Warren, J. A.; Hayes, J. M.; Small, G. J. *J. Chem. Phys.* **1984**, *80*, 1786.

(43) Wunsch, L.; Metz, F.; Neusser, H. J.; Schlag, E. W. *J. Chem. Phys.* **1977**, *66*, 386.

(44) Small, G. J.; Burke, F. P. *J. Chem. Phys.* **1977**, *66*, 1767.

(45) Burke, F. P.; Eslinger, D. R.; Small, G. J. *J. Chem. Phys.* **1975**, *63*, 1309.

(46) Lacey, A. R.; McCoy, E. F.; Ross, I. G. *Chem. Phys. Lett.* **1973**, *21*, 233.

(47) Small, G. J. *J. Chem. Phys.* **1971**, *54*, 3300.

(48) Santoro, F.; Improta, R.; Lami, A.; Bloino, J.; Barone, V. *J. Chem. Phys.* **2007**, *126*, 84509.

(49) Santoro, F.; Lami, A.; Improta, R.; Barone, V. *J. Chem. Phys.* **2007**, *126*, 184102.

(50) Santoro, F.; Lami, A.; Improta, R.; Bloino, J.; Barone, V. *J. Chem. Phys.* **2008**, *128*, 224311.

(51) Yan, Y. J.; Mukamel, S. *J. Chem. Phys.* **1986**, *85*, 5908.

(52) Tang, J.; Lee, M. T.; Lin, S. H. *J. Chem. Phys.* **2003**, *119*, 7188.

(53) Ianconescu, R.; Pollak, E. *J. Phys. Chem. A* **2004**, *108*, 7778.

(54) Lin, S. H. *J. Chem. Phys.* **1966**, *44*, 3759.

(55) Lin, S. H. *J. Chem. Phys.* **1970**, *53*, 3766.

(56) Lin, S. H. *J. Chem. Phys.* **1972**, *56*, 2648.

(57) Lin, S. H. *J. Chem. Phys.* **1973**, *58*, 5760.

(58) Deng, C.; Niu, Y.; Peng, Q.; Shuai, Z. *Acta Phys. Chim. Sin.* **2010**, *26*, 1051.

(59) Eckart, C. *Phys. Rev.* **1935**, *47*, 552.

(60) Wilson, E. B., Jr.; Decius, J. C.; Cross, P. C. *Molecular Vibrations*; McGraw-Hill: New York, 1955.

(61) Dymarsky, A. Y.; Kudin, K. N. *J. Chem. Phys.* **2005**, *122*, 124103.

(62) Dibartolo, B. *Radiationless Processes*; Plenum Press: New York, 1980.

(63) Tang, J.; Lin, S. H. *Phys. Rev. E* **2006**, *73*, 61108.

(64) Lengsfield, B. H., III; Saxe, P.; Yarkony, D. R. *J. Chem. Phys.* **1984**, *81*, 4549.

(65) Send, R.; Furche, F. *J. Chem. Phys.* **2010**, *132*, 44107.

(66) Tavernelli, I.; Tapavicza, E.; Rothlisberger, U. *J. Chem. Phys.* **2009**, *130*, 124107.

(67) Hu, C.; Sugino, O.; Tateyama, Y. *J. Chem. Phys.* **2009**, *131*, 114101.

(68) Hu, C.; Hirai, H.; Sugino, O. *J. Chem. Phys.* **2007**, *127*, 64103.

(69) Tapavicza, E.; Tavernelli, I.; Rothlisberger, U. *Phys. Rev. Lett.* **2007**, *98*, 23001.

(70) Billeter, S. R.; Egli, D. *J. Chem. Phys.* **2006**, *125*, 224103.

(71) Billeter, S. R.; Curioni, A. *J. Chem. Phys.* **2005**, *122*, 34105.

(72) Baer, R. *Chem. Phys. Lett.* **2002**, *364*, 75.

(73) Tommasini, M.; Chernyak, V.; Mukamel, S. *Int. J. Quantum Chem.* **2001**, *85*, 225.

(74) Chernyak, V.; Mukamel, S. *J. Chem. Phys.* **2000**, *112*, 3572.

(75) Deglmann, P.; Furche, F. *J. Chem. Phys.* **2002**, *117*, 9535.

(76) Deglmann, P.; Furche, F.; Ahlrichs, R. *Chem. Phys. Lett.* **2002**, *362*, 511.

(77) Treutler, O.; Ahlrichs, R. *J. Chem. Phys.* **1995**, *102*, 346.

(78) Furche, F.; Ahlrichs, R. *J. Chem. Phys.* **2002**, *117*, 7433.

(79) Becke, A. D. *J. Chem. Phys.* **1993**, *98*, 5648.

(80) Stephens, P. J.; Devlin, F. J.; Chabalowski, C. F.; Frisch, M. J. *J. Phys. Chem.* **1994**, *98*, 11623.

(81) Schafer, A.; Horn, H.; Ahlrichs, R. *J. Chem. Phys.* **1992**, *97*, 2571.

(82) Koch, W.; Holthausen, M. C. *A Chemist's Guide to Density Functional Theory*; 2nd ed.; Wiley-VCH Verlag GmbH: Berlin, 2001; p 134.

(83) Frisch, M. J.; Trucks, G. W.; Schlegel, H. B. *Gaussian 03*; Gaussion Inc.: Pittsburgh, PA, 2003.

(84) Furche, F. *J. Chem. Phys.* **2001**, *114*, 5982.

(85) Johnson, B. G.; Gill, P. M. W.; Pople, J. A.; Fox, D. J. *Chem. Phys. Lett.* **1993**, *206*, 239.

(86) Frigo, M.; Johnson, S. G. *Proc. IEEE* **1962**, *93*, 216.

(87) Gouterman, M. In *The Porphyrins*; Dolphin, D., Ed.; Academic Press: New York, 1977; Vol. 3.

(88) Edwards, L.; Dolphin, D. H.; Gouterman, M.; Adler, A. D. *J. Mol. Spectrosc.* **1971**, *38*, 16.

(89) Edwards, L.; Dolphin, D. H.; Gouterman, M. *J. Mol. Spectrosc.* **1970**, *35*, 90.

(90) Seda, J.; Burda, J. V.; Leszczynski, J. *J. Comput. Chem.* **2005**, *26*, 294.

(91) Gouterman, M. *J. Chem. Phys.* **1959**, *30*, 1139.

(92) Gouterman, M.; Wagnière, G. H.; Snyder, L. C. *J. Mol. Spectrosc.* **1963**, *11*, 108.

(93) Reimers, J. R. *J. Chem. Phys.* **2001**, *115*, 9103.

(94) Anthony, J. E. *Chem. Rev.* **2006**, *106*, 5028.

(95) Lehnherr, D.; Gao, J.; Hegmann, F. A.; Tykwinski, R. R. *Org. Lett.* **2008**, *10*, 4779.

(96) Platt, A. D.; Day, J.; Subramanian, S.; Anthony, J. E.; Ostroverkhova, O. *J. Phys. Chem. C* **2009**, *113*, 14006.

(97) Wolak, M. A.; Delcamp, J.; Landis, C. A.; Lane, P. A.; Anthony, J.; Kafafi, Z. *Adv. Funct. Mater.* **2006**, *16*, 1943.

(98) Wolak, M. A.; Melinger, J. S.; Lane, P. A.; Palilis, L. C.; Landis, C. A.; Delcamp, J.; Anthony, J. E.; Kafafi, Z. H. *J. Phys. Chem. B* **2006**, *110*, 7928.

(99) Nijegorodov, N.; Ramachandran, V.; Winkoun, D. P. *Spectrochim. Acta Part A* **1997**, *53*, 1813.

(100) Platt, J. R. *J. Chem. Phys.* **1949**, *17*, 484.

(101) Dierksen, M.; Grimme, S. *J. Chem. Phys.* **2004**, *120*, 3544.

Feature Article

*J. Phys. Chem. A, Vol. 114, No. 30, 2010* **7831**

(102) Ferguson, J.; Reeves, L. W.; Schneider, W. G. *Can. J. Chem.* **1957**, *35*, 1117.

(103) Lambert, W. R.; Felker, P. M.; Zewail, A. H. *J. Chem. Phys.* **1981**, *75*, 5958.

(104) Petrenko, T.; Krylova, O.; Neese, F.; Sokolowski, M. *New J. Phys.* **2009**, *11*, 15001.

(105) Banasiewicz, M.; Deperasinska, I.; Kozankiewicz, B. *J. Phys. Chem. A* **2003**, *107*, 662.

(106) Beer, M.; Longuet-Higgins, H. C. *J. Chem. Phys.* **1955**, *23*, 1390.

(107) Viswanath, G.; Kasha, M. *J. Chem. Phys.* **1956**, *24*, 574.

(108) Rentzepis, P. M. *Chem. Phys. Lett.* **1968**, *2*, 117.

(109) Rentzepis, P. M. *Chem. Phys. Lett.* **1969**, *3*, 717.

(110) Hochstrasser, R. M.; Li, T. *J. Mol. Spectrosc.* **1972**, *41*, 297.

(111) Ippen, E. P.; Shank, C. V.; Woerner, R. L. *Chem. Phys. Lett.* **1977**, *46*, 20.

(112) Huppert, D.; Jortner, J.; Rentzepis, P. M. *J. Chem. Phys.* **1972**, *56*, 4826.

(113) Amirav, A.; Jortner, J. *J. Chem. Phys.* **1984**, *81*, 4200.

(114) Fiedler, S. E.; Hoheisel, G.; Ruth, A. A.; Hese, A. *Chem. Phys. Lett.* **2003**, *382*, 447.

(115) Lou, Y.; Chang, J.; Jorgensen, J.; Lemal, D. M. *J. Am. Chem. Soc.* **2002**, *124*, 15302.

(116) Gustav, K.; Storch, M. *Int. J. Quantum Chem.* **1990**, *38*, 1.

(117) Englman, R.; Jortner, J. *Mol. Phys.* **1970**, *18*, 145.

(118) Gillispie, G. D.; Lim, E. C. *Chem. Phys. Lett.* **1979**, *63*, 193.

(119) Griesser, H. J.; Wild, U. P. *Chem. Phys.* **1980**, *52*, 117.

(120) Siebrand, W. *J. Chem. Phys.* **1967**, *47*, 2411.

(121) Schlag, E. W.; Schneider, S.; Fischer, S. F. *Annu. Rev. Phys. Chem.* **1971**, *22*, 465.

(122) Siebrand, W. *J. Chem. Phys.* **1967**, *46*, 440.

(123) Tatchen, J.; Pollak, E. *J. Chem. Phys.* **2009**, *130*, 41103.

(124) Levine, B. G.; Coe, J. D.; Virshup, A. M.; Martínez, T. J. *Chem. Phys.* **2008**, *347*, 3.

(125) Zhu, C.; Liang, K. K.; Hayashi, M.; Lin, S. H. *Chem. Phys.* **2009**, *358*, 137.